Diffusion processes in copper-nickel-tin system.

Ogbunugafor Anthony E.∗1, Lekeka Biniam B.†2, Tyohule Philip Aondongu.1, and Eshetu mintesenot A.1,

[1]Department of Advanced Materials Science, MISIS University, RUSSIA

ABSTRACT

This research is a detailed investigation of the diffusion processes in binary Cu-Ni and ternary Cu-Sn-Ni systems, primarily focusing on comprehending the phase evolution, diffusion behavior, and microstructural development under controlled thermal conditions. Mass transport processes and phase formation are described in these systems. Comparing the diffusion process in Cu-Sn/Ni and Cu/Ni is the main purpose of this work, which involves sample preparation, diffusion annealing, and then examining and characterizing their final states with light microscopy, scanning electron microscopy, and energy-dispersive X-ray spectroscopy (EDS). Analysis Cu of–Ni and Cu-Sn interdiffusion profiles. The profile illustrates a classic interdiffusion pattern between diffusion couples. The diffusion coefficient of Cu in the Cu-rich zone D_{Cu} was 8.36E-04 m^2/s, while those of Ni in the Ni-rich zone and Cu-Sn zones were 4.17E-04 □m^2/s and 4.875E-03 m^2/s, respectively. The higher diffusion coefficient of Cu-Sn suggests greater atomic mobility in Cu-Sn is due to higher vacancy concentration and lattice distortion for Sn atoms.

This thesis consists of an introduction …48.. pages, 12 conclusions. In includes …31. Figures, 3…. tables, …53. References.

INTRODUCTION

Diffusion is fundamental in materials science and is used in metallurgical joints and maintaining the stability of electronic packaging for a long time. This process includes the atomic movement of constituent elements along the compositional gradient in a structure, which leads to the growth of intermetallic compounds and the evolution of a complex microstructure. Such diffusion-driven changes have major effects on the mechanical integrity, thermal stability, electrical properties, and overall performance of materials.

Both Cu–Ni and Cu-Sn-Ni metallic systems play key roles in microelectronics, solder use, and high-temperature component design. Because both Cu and Ni are essential for their conductivity and strength, respectively, their solid solution is incomplete, making the Cu-Ni system a leading example for probing diffusion. Meanwhile, the Cu-Sn-Ni system includes several IMCs, along with variations in diffusivity and phase transformations that have a significant effect on the performance and failure of solder joints in high-tech electronics. Creating Cu_6Sn_5, Cu_3Sn and Ni_3Sn_4 intermetallic compounds, their growth rate and

simultaneous ballooning of the Kirkendall voids cause embrittlement, delamination and device failure. Detailed knowledge of how these substances behave and spread is needed to ensure the stability of the contacts and to select the most suitable assembly materials. The reliability of Cu-based electronic devices is now at risk because of the interdiffusion and phase changes at their interfaces due to device shrinkage and higher operating temperatures. Nonetheless, the focus on the bronze system is primarily on its industrial significance, yet what matters most here is to show how diffusion takes over in solid-solution systems.

At one hand the systems Cu-Ni, Cu-Sn and Ni-Sn were studied before by a number of authors. A short description of the main results is provided in the literature review. However, for 3 component system, the situation becomes more difficult and some contradictions in the results can be observed. At a minimum, it is concerned with the possible phase formation and growth rate.

Here, we focus on the formation of intermediate phases and possible mass transport through the interface.

1 Analytical Literature Review

This review examines previous studies on diffusion, phase formation, thermodynamic processes, and microstructural growth in Cu-Ni and Cu-Sn-Ni systems. This review identified important knowledge gaps based on analyzing theoretical models, carrying out simulations, and examining the results from experiments.

1.1 Definition of Diffusion

Diffusion refers to the movement of atoms, molecules, or small particles from a region of higher concentration to a region of lower concentration because of random motion. Brownian motion or diffusion helps small particles (<0.1 µm) or molecules travel when there is no convection and the distance they need to move is a few millimeters or less. Moving materials over great distances with diffusion can take a long time, and other factors, such as convection, become necessary to quickly move materials sufficiently in a reasonable period of time (i.e., within one day).

1.2 Laws of Diffusion

The principles of diffusion were often explained using the theory of Adolf Fick in 1855. These laws provide a way to measure how quickly the diffusive flux changes based on variations in concentration and time. They can be used to calculate the diffusion coefficient Di. Fick's first law can be used to derive his second law, which is identical to the diffusion equation.

1.2.1 Fick's First Law

Fick's first law relates the diffusive flux to the concentration gradient. It states that the flux moves from regions of higher concentration to regions of low concentration, with a magnitude that is proportional to the concentration gradient. [7, 8] In one dimension, the law can be written as:

$$j_i = -D_i \frac{\partial c_i}{\partial x}.$$

(1).

where,

Ji is the diffusion flux (mol/m^{2}s)

Ji measures the amount of substance flowing through a unit area during a unit time interval.

Di is the diffusion coefficient (m^2/s)

$\frac{\partial c_i}{\partial x}$. where, is the concentration gradient.

Ci is the concentration of diffusing species (mol/m^3)

x is spatial co-ordinate (m)

The negative sign (-) indicates that diffusion occurs down the concentration gradient, moving from regions of high concentration to a region of low concentration [9]

In two or more dimensions we use □□□the del or gradient operator, which generalizes the first derivative, obtaining

$$\mathbf{j_i} = -M_i \nabla \ln c_i = -\frac{M_i}{c_i} \nabla c_i = D_i \nabla c_i \quad \text{----------(2)}$$

where,

Ji is the diffusion flux (amount of substance per unit area per unit time, mol/m^2.s)

The driving force for the one-dimensional diffusion is the quantity $\frac{\partial c_i}{\partial x}$, which where, is the concentration gradient.

1.2.2 Fick's Second Law

Fick's second law predicts how diffusion causes concentration to change with respect to time. [11] It is a partial differential equation that states in one dimension:

$$\frac{\partial c}{\partial t} = D \frac{\partial^2 c}{\partial x^2}.$$

(3)

where *C* is the concentration (mol/m3);

C= *C*(*x*,*t*) is a function that depends on location (*x*) and time (*t*);

t is time (s);

x is the position (m).

In two or more dimensions we use the laplacian Ñ = Ñ2, which generalises the secondderivatives, to obtain the equation: $\frac{\partial c}{\partial t} = D\Delta c,$

(4)

Fick's second law has the same mathematical form as the Heat equation and its fundamental solution is the same as the Heat kernel, except switching thermal conductivity k with diffusion coefficient D: [11]

$$C(x,t) = \frac{1}{\sqrt{4\pi Dt}} \exp\left(-\frac{x^2}{4Dt}\right).$$

(5)

Fick's diffusion equation is useful for modelling phase transformations, chemical reactions, and interdiffusion in alloys. However, the solution depends on the initial distribution of elements and boundary conditions.

1.2.3 Diffusion Coefficient (D)

The diffusion coefficient, also known as the diffusivity, quantifies the rate at which the species diffuses. This is the proportionality constant between the molar flux due to molecular diffusion and the negative value of the gradient in the concentration of the species. In other words, it is a proportionality factor in Fick's law and depends on the nature of the diffusing species, medium, and temperature. The diffusivity has dimensions of length2 / time, or m2/s) in SI units and cm2/s in CGS units.

Factors Affecting Diffusivity (D)

I. Temperature: Typically follows an Arrhenius-type behavior:

$$D = D_0 \exp\left(-\frac{E_A}{RT}\right)$$

(6)

Where

D is the diffusion coefficient (in m2/s),

D_0 is pre-exponential factor (D value at infinite temperature; in m2/s),

E_A is the activation energy for diffusion (in J/mol),

T is the absolute temperature (in K),

R ≈ 8.314 J/(mol.K) was the universal gas constant.

11. Crystal Structure: Diffusion is faster in BCC than in FCC owing to the lower packing density.

lll. Concentration of Defects: Higher vacancy concentration increased diffusion.

lV. Diffusing species: Larger or heavier atoms diffuse more slowly.

There are three distinct methods to determine the diffusion coefficient, which correspond to three different types of diffusion processes [10].

1. Self Diffusion

Because atoms are usually indisquishable, we can monitor the diffusion of a diffusant, which is a radioactive isotope (^{63}Ni), with a material made of naturally occurring material (^{Nat}Ni). This type of experiment usually entails wrapping the stable isotope (^{Nat}Ni) with a film of radioactive isotope (^{63}Ni) and then observing the concentration of the radioactive isotope as it diffuses into the sample. Because stable and radioactive isotopes have almost identical physical and chemical characteristics, this process is known as self-diffusion[10].

2. Hetero-diffusion

Diffusion of one molecular species with another, such as Ni, in Cu. By coating a large Cu sample with a Ni diffusant film and observing the Ni concentration profile in Cu, this type of diffusion can occur. Since Ni and Cu have different electronegativity and atomic radii, diffusion is affected by atomic interactions.[10]

3. Mutual Diffusion

This type of diffusion occurs when two species diffuse, thereby establishing a compositional gradient. This can be observed by joining two large Ni and Cu samples together at high temperatures, leading to the gradual formation of a Cu-Ni solid solution and the Ni and Cu composition profiles on both sides of the interface can be.[10]

1.3 Mechanisms of Diffusion

Diffusion occurs when atoms or molecules move from regions of high to regions of low concentration due to thermal energy.[2] Atomic movement is important for alloy homogenization, precipitation strengthening, and high-temperature performance. The movement of atoms in solid ia is a result of various diffusion mechanisms, mainly due to temperature, atomic size, crystal structure, and the presence of defects. Diffusion is a basic process in metals and alloys that governs their microstructural evolution, phase transformation, and mechanical properties. [1] The primary diffusion mechanisms include the following.

1. Vacancy Diffusion
2. Interstitial Diffusion
3. Grain boundary Diffusion
4. Dislocation Diffusion

Temperature, crystal structure, and atomic size are factors that affect each mechanism.

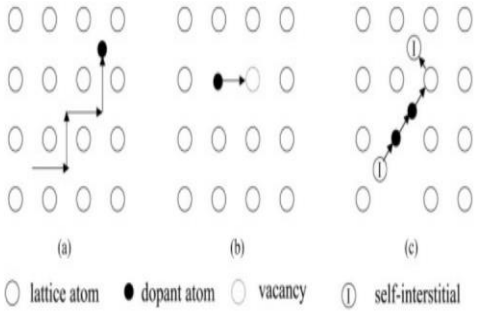

Figure 1 – Diffusion Mechanism in two-dimensional lattice, (a) Interstitial Mechanism, (b) Vacancy Mechanism, (c) Interstitially Mechanism [1]

1.3.1. Vacancy Diffusion

The most common diffusion mechanism in substitutional alloys, such as Cu-Ni and Cu-Sn-Ni, is vacancy diffusion. In this process, atoms move by exchanging places with the vacant lattice sites (vacancies). An atom can effectively move into a vacant lattice site, causing the atom and vacancy to switch places. If large-scale diffusion occurs in a metal, there is a flux of atoms in one direction and a flux of vacancies in the other direction. [3, 4] A vacancy can have its own diffusion coefficient that is expressed as:

$$D_v = \frac{1}{6}\alpha^2\Gamma_v \quad (7)$$

Where,

Γ_v where is the jump frequency of vacancy.

α is the jump distance

Observation in Cu-Ni and Cu-Sn-Ni Systems

Vacancy diffusion plays the main role in Cu-Ni systems because of the equal atomic radii of Cu and Ni, which enables the atoms to swap positions with minimal lattice strain.

Because Sn has a larger atomic size and lower diffusivity, the presence of Sn in the Cu-Sn-Ni system creates a vacancy diffusion complex, resulting in the formation of different phases and diffusion anisotropy.

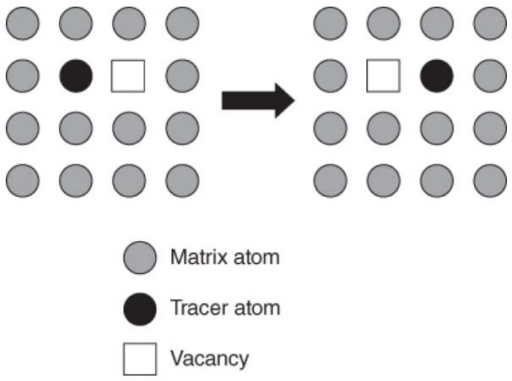

Figure 2 – Schematic Representation of vacancy diffusion in FCC metals

1.3.2 Interstitial Diffusion

A diffusant (carbon, hydrogen, or nitrogen) in interstitial diffusion diffuses between the lattice structures of other crystalline elements. Interstitial diffusion does not require the presence of vacant lattice sites, making it much faster. [4] The movement of atoms can be described as jumps, and the interstitial diffusion coefficient depends on the jump frequency. The jump frequency G is given by

$$\Gamma = zv\exp\left(\frac{-\Delta G_m}{RT}\right) \quad (8)$$

Where,

z is the number of nearest-neighboring interstitial sites.

v is vibration frequency of the interstitial atom due to thermal energy

ΔG_m is the activation energy for the migration of the interstitial atoms between sites

Observation in Cu-Ni and Cu-Sn-Ni Systems

The Cu-Ni system has a complete solid solubility and is a substitutional binary system. Cu and Ni

have similar radii (128 pm and 124 pm, respectively), crystal structures, valences, and electronegativities. No interstitial diffusion occurs with Cu or Ni as their atomic sizes are similar and the alloys have full solubility with no interstitial elements.[41]

Studies on self-diffusion and impurity diffusion indicate that Ni diffuses slightly faster in Cu than in Ni at high temperatures.

In the Cu-Sn-Ni system, the Sn atoms are larger (atomic radii of 140 pm), making interstitial diffusion unlikely in Cu or Ni. The growth of intermetallic compounds, such as Ni3Sn4 and Cu6Sn5, in the Cu-Sn-Ni diffusion couple indicates dominant substitutional diffusion. The interstitial diffusion of Cu and Sn has not been observed directly, but abnormal diffusion profiles suggest their occurrence. [41,42] However, Interstitial diffusion can alter the mechanical properties of these alloys, resulting in embrittlement when impurities, such as hydrogen, are present.

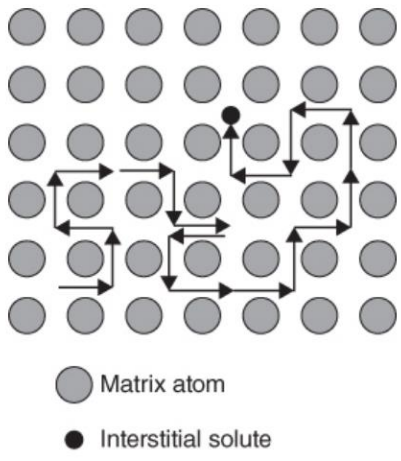

Figure 3 Interstitial Diffusion Mechanism in FCC lattice.

1.3.3. Grain Boundary Diffusion

Grain boundary diffusion occurs along the interfaces between grains in polycrystalline materials. Because atomic packing is less dense at the grain boundaries, diffusion is significantly faster than through the bulk lattice. Fisher suggested a general method to evaluate the grain boundary diffusion [5]. In the Fisher model, the grain boundary is represented as a thin layer of a high-diffusivity uniform and isotropic slab embedded in a low-diffusivity isotropic crystal. If the thickness of the slab is δ, the length is y, and the depth is a unit length, the diffusion process can be described as the following formula: [4, 5]

$$\frac{\partial c}{\partial t} = D\left(\frac{\partial^2 c}{\partial x^2} + \frac{\partial^2 c}{\partial y^2}\right) \text{ where } |x| > \delta/2 \quad (9)$$

This equation represents diffusion in the volume.

$$\frac{\partial c_b}{\partial t} = D_b\left(\frac{\partial^2 c_b}{\partial y^2}\right) + \frac{2D}{\delta}\left(\frac{\partial c}{\partial x}\right)_{x=\delta/2} \quad (10)$$

This equation represents the diffusion along the grain boundary.

where:

C(x,y,t) is the volume concentration of the diffusing atoms

C_b(y,t) is the concentration at the grain boundary.

Observation in Cu-Ni and Cu-Sn-Ni Systems

In the Cu-Sn-Ni system, the presence of intermetallic phases leads to their formation at the grain boundaries, which makes grain boundary diffusion important in the system.

In the Cu-Ni system, grain boundary diffusion becomes significant at high temperatures (>900k), influencing the phase homogenization.

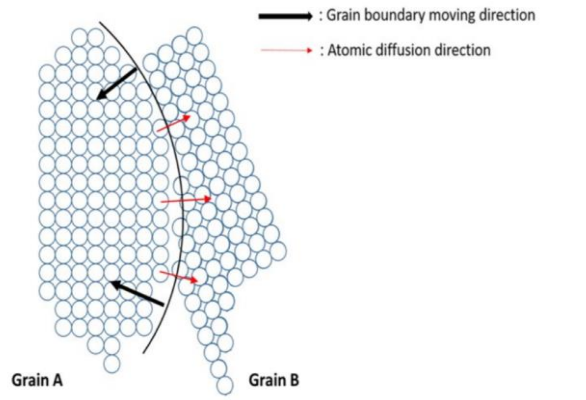

Figure 4 – Diagram of grain boundary diffusion by atomic transition from grain A to grain B

1.3.4 Dislocation Diffusion

Diffusion in dislocations is a short-circuit diffusion, often referred to as pipe diffusion. Dislocation diffusion occurs when adjacent sub-units of a cluster move in a row-by-row fashion through dislocation displacement. The process begins with nucleation of the dislocation, followed by sequential displacement on a concerted basis. Diffusion in dislocations depends on the density of the dislocations in the materials being studied. [6]

Dislocations provide fast diffusion paths owing to their high free volume and low activation energy for atomic movement.

Observation in Cu-Ni and Cu-Sn-Ni Systems

In cold-worked Cu-Ni systems showing non-Fickian diffusion profiles, dislocation diffusion becomes more prominent owing to the increased density of dislocations.

In the Cu-Sn-Ni system, dislocations are generated during IMC growth, thermal cycling, and plastic deformation of the solder joints. In Cu-Sn-Ni alloys, dislocation diffusion contributes to the creep deformation and stress relaxation.

1.4 Darken's Analysis

The Darken equation was used to describe the solid-state diffusion of the materials in binary solutions. This equation was first described by Darken in 1948 [12]. This equation is applied to cases where the two components of the solid solution do not have the same coefficient of diffusion. Darken's first equation is: [12]

$$\nu = (D_1 - D_2)\frac{\partial N_1}{\partial x} = (D_2 - D_1)\frac{\partial N_2}{\partial x}.$$

(11)

where,

v is the marker velocity of inert markers showing the diffusive flux.

D_1 and D_2 are the diffusion coefficients of the two components, respectively.

N_1 and N_2 are the atomic fractions of the two components, respectively.

x represents the direction in which the diffusion was measured.

It is important to note that this equation only holds in conditions where the total concentration remains constant.

Darken's Second equation is:

$$\tilde{D} = (N_1 D_2 + N_2 D_1)(1 + N_1 \frac{\partial \ln a_1}{\partial \ln N_1}).$$

(12).

where,

a_1 is the activity coefficient of the first component

where D denotes the overall diffusivity of the binary solution.

Darken cited Simgelskas and Kirkendell's experiment, which examined the mechanisms and rates of diffusion and produced a concept known as the Kirkendall effect [13].

The experiment involved placing inert molybdenum wires at the interface between copper and brass components and tracking the motion of the markers. The experiment validated the concept that a concentration gradient in a binary alloy would result in components with different velocities in the solid solution.

The experiment demonstrated that because the molybdenum wires move deeper into the brass, zinc has a higher relative velocity than copper. In establishing the coordinate axes to evaluate the derivation, Darken cited back to Smigelskas and Kirkendall's experiment, in which inert wires were labelled as the origin [12, 13].

In order to derive the second equation, Darken et al.. Johnson's experiment on a gold-silver system was conducted to determine the chemical diffusivity. In this experiment, radioactive gold and silver isotopes were used to evaluate the diffusivity of gold and silver, since radioactive isotopes were assumed to have the same mobility as non-radioactive elements. If the gold-silver solution is assumed to behave ideally, it would be expected that the diffusivities would also be equivalent. Consequently, the overall diffusion coefficient of the system would be the average of the diffusivity of each component; unfortunately, this was not the case. As a result of this discovery, Darken analyzed Johnson's experiment and proposed a formula for the chemical diffusivity of binary solutions.

1.4.1 Kirkendall Effect

The Kirkendall effect is the movement of the interface between two metals that occurs because of variations in the diffusion rates of the metal atoms. When insoluble markers are placed at the interface between a pure metal and an alloy containing the metal and heated to a temperature where atomic diffusion is reasonable for the specified duration, the boundary moves relative to the markers. [12]

This process was named in honor of Ernest Kirkendall (1914-2005), an assistant processor of chemical engineering at Wayne State University from to 1941-1946.

The Kirkendall effect has significant practical implications. One of these is the prevention or suppression of voids that occur at the boundary interface in different types of alloy–metal bonding. These are referred to as Kirkendall voids (KVs).

In the Kirkendall experiment, a bar of brass (70% Cu, 30% Zn) served as the core, with molybdenum wires stretched along its length, and then coated with a layer of pure copper. Molybdenum was used as the marker material because it is very insoluble in brass, eliminating any errors caused by the markers diffusing on their own. Diffusion was allowed to take place at 785^0C for a period of 56 days, and cross-sections were obtained six times throughout the experiment. It was observed that the wire markers moved closer together as zinc diffused out of the brass and into copper. A difference in the location of the interface was visible in the cross-sections at different times. Using X-ray diffraction, the compositional change of the material due to diffusion was verified [12].

From this study, two conclusions were drawn that had a significant influence on solid-state diffusion:

1. The rate of diffusion of zinc is much greater than that of copper in brass
2. When Zn diffuses more rapidly than Cu, the

interface shifts to compensate, at least partially, for the diffusion rate.

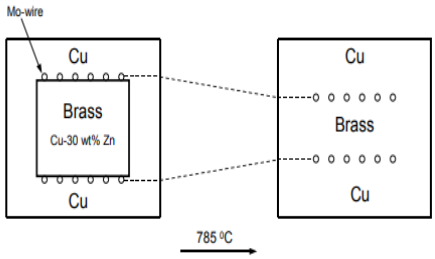

Figure 5 – Schematic representation of a cross-section of diffusion couples prepared by Smigelkas and Kirkendall before and after annealing at 7850C. The molybdenum wires moved closer to each other over time.

Observations of the Kirkendall Effect in Cu-Ni and Cu-Sn-Ni Systems

The Kirkendall effect provides experimental proof of the unequal diffusion rates in binary systems. In the Cu-Ni couple, Cu diffuses faster than Ni, and inert markers positioned at the interface move toward the Ni side, which diffuses more slowly. Additionally, this phenomenon leads to the formation of vacancies and occasionally voids at the interface.

1.5 Interdiffusion in Binary System: Cu-Ni alloys

1.5.1 Historical Studies of Diffusion

For more than a century, solid-state physics, metallurgy, and material science specialists have studied diffusion in the Cu-Ni system. Because Cu-Ni alloys are needed for various high-temperature applications, coinage, and corrosion-resistant materials, researchers have investigated the mechanism of diffusion in Cu-Ni alloys. This review covers the historical background of diffusion research, with an emphasis on key experimental contributions and theoretical advancements.

1. Early Observations and Pre-Theoretical Era (Pre-19th Century)

While diffusion was not be clearly defined as a phenomenon, ancient scientists observed natural diffusion such as aromas mingling, salt in water, and color dispersion in solution [15]. An example, when science and mathematics could not be used, Greek philosophers expressed opinions on the behavior of atoms. By studying color mixing and additive reactions in solutions, alchemists and early chemists suggested a type of mass movement.

However, these discoveries remain qualitative in the absence of a theoretical or mathematical framework.

2. Metallurgical Origins (19th Century)

The first real encounter with diffusion in solids was in metallurgy and blacksmithing, when artisans observed that heating metals caused changes in their composition and hardness at the surface. The observations, however, suggested the importance of mass transport, but the details of the process are still unclear in atomic terms.

I. Robert Austen (1896)

Austen observed that when steel is exposed to carbon through heat, carbon diffuses into the metal and creates carburized layers at the surface. This was an early observation of interstitial diffusion.

II Carburization and Decarburization

By the late 1800s, engineers had begun to control diffusion without fully understanding the principles when they realized that carbon may diffuse into or out of steel after heat treatment, resulting in different mechanical properties.

3. Quantitative Theory and Breakthrough Experiments (20th Century)

I. Fick's Laws Applied to Solids

Although Adolf Fick formulated his laws of diffusion in 1855 for liquids, it was not until the early 20th century that researchers began extending these equations to solid-state diffusion: Fick's steady-state first law

$$j_i = -D_i \frac{\partial c_i}{\partial x}.$$

Fick's Second Law (Non-Steady State):

$$\frac{\partial c}{\partial t} = D \frac{\partial^2 c}{\partial x^2}.$$

Here, D is the diffusion coefficient, which is a key material property that is dependent on the temperature and atomic structure.

4. Landmark Experiments

I. Le Claire and Seith (1930s–1940s)

The introduction of isotopic 'markers' into metals and following their movement with tracer diffusion techniques which made it possible to quantify diffusion coefficients in metals like nickel, copper and zinc.

II Paul Kirkendall (1947)

The discovery of the Kirkendall Effect is one of the main results of studies on diffusion. Initially, inert markers were used to mark the Cu–Zn diffusion couple interface. The fact that the markers shifted following annealing indicated that, unlike what was expected before, atoms of different metals have different diffusion rates during annealing. Proved that that diffusion works through vacancy migration, revolutionizing the understanding of diffusion in solids.

III Georg Hevesy and Fritz Paneth (1920s):

Used special radioactive tracers to compare metal diffusion under different conditions.

IV Darken's Equations (1948):

Used thermodynamic arguments to elaborate on interdiffusion in binary alloys, including ideas like intrinsic and interdiffusion coefficients.

V Shewmon, Mehrer, and Paul (1950s–2000s):

Contributed a lot to the experiments and theoretical modeling of solid-state diffusion.[15]

5. Modern Theoretical and Computational Approaches (Late 20th – 21st Century)

With advancements in computing and characterization of materials, diffusion studies are now able to address: Atomistic models like Molecular Dynamics and Kinetic Monte Carlo which simulate atoms by atom moving point to point and forecast the diffusion behavior at nanoscale.

With Phase Field Modeling, the diffusion of various materials in multi-phase and multi-component systems can be analyzed.

Ab Initio and Density functional theory (DFT) methods help you calculate the energy migration and the diffusion barriers at atomic scales.

Recent Focus Areas:

1. Diffusion in nanomaterials: Due to increased grain boundary and surface diffusion.
2. Ionic diffusion in batteries: Mainly in Li-ion, Na-ion and solid-state electrolytes.
3. Diffusion in nuclear and space materials: Radiation causes substantial diffusion in nuclear and space materials.

4. Diffusion under extreme conditions: caused by high pressure, stress or magnetic fields.

6. Experimental Advances in Diffusion Studies

1. Modern experimental techniques have revolutionized diffusion measurements:
2. Secondary Ion Mass Spectrometry (SIMS)
3. Electron Probe Microanalysis (EPMA)
4. Time-of-Flight Secondary Ion Mass Spectrometry (TOF-SIMS)
5. Atom Probe Tomography (APT)
6. In-situ TEM and 3D tomography

These enable the tracking of diffusion at atomic or nanometer scales because to their excellent spatial and compositional resolution.

8. An Evolving Discipline:

From the 19th-century descriptions based on experiments to the 21st-century multiscale, the study of diffusion has evolved a lot. Many fields now rely on the use of statistics, for example:

1. Materials design
2. Semiconductor manufacturing
3. Biomaterials and tissue engineering
4. Energy storage and conversion (batteries, fuel cells)
5. Environmental and geological systems

As diffusion theory has progressed from Graham and Fick through Einstein, Kirkendall and modern engineers and scientists, it shows how interdisciplinary discoveries have continuously improved our comprehension of this basic physical phenomenon.[15]

1.6 Typical solutions of diffusion equation.

Case 1: Instantaneous point source in an infinite medium [10]

Solution:

$$c(x,t) = \frac{q}{2\sqrt{\pi Dt}} e^{-x^2/4Dt},$$

(13)

Initial Condition:

$$c(x, 0) = q.\ \delta(x)$$

δ(x) is the Dirac function, representing an instantaneous injection of mass at a single point x=0.

Here, no boundary constraints since it's an infinite medium (x Î (-¥, ¥)).

Case 2: Semi-infinite medium with constant surface concentration[10]

Solution:

$$c(x,t) = c_s \text{erf}\, c\left(\frac{x}{2\sqrt{Dt}}\right)$$

(14)

Initial condition:

C(x,0) = 0 for x>0

Boundary condition:

1. C(0,t) = Cs (surface at x = 0 maintained at concentration Cs)
2. C(□ □t) = 0

Case 3: Semi-infinite medium initially saturated with Cs, surface suddenly exposed to vacuum[10]

Solution:

$$c(x,t) = c_s \text{erf}\left(\frac{x}{2\sqrt{Dt}}\right)$$

(15)

Initial Condition:

C(x,0) = Cs for x > 0

Bounndary Condition:

1. C(0,t) = 0 (instantaneous sink at surface)
2. C(0,t) = Cs

Case 4: Infinite medium, Instantaneous surface source[10]

Solution:

$$c(x,t) = \frac{c_s}{2}\text{erf}\,c\left(\frac{x}{2\sqrt{Dt}}\right)$$

(16)

Initial Condition:

C(x,0) = 0

Boundary Condition:

An instantaneous introduction of surface concentration that is not maintained (e.g deposition of atoms on a surface at t = 0)

Case 5: Infinite Medium with surface concentration jump and interior initially uniform.[10]

Solution:

$$c(x,t) = \frac{c_s}{2}\left[1 + \text{erf}\left(\frac{x}{2\sqrt{Dt}}\right)\right]$$

(17)

Initial Condition:

C(x,0) = 0 for x<0; C(x,0) = Cs for x>0

Boundary condition:

1. No specific boundary at x = 0, but the condition is symmetric around it.

Case 6: Semi-Infinite with finite layer of width 2a

Solution:

$$c(x,t) = \frac{c_s}{2}\left[\text{erf}\left(\frac{a+x}{2\sqrt{Dt}}\right) + \text{erf}\left(\frac{a+x}{2\sqrt{Dt}}\right)\right]$$

(18)

Initial Condition:

$$C(x,0) = \begin{cases} C_s, & -a < x < a \\ 0, & \text{otherwise} \end{cases}$$

Boundary Condition:

1. Diffusion occurs into surrounding media
2. No surface constraints beyond the finite layer

Case 7: Finite plate (slab) of thickness 2L with constant surface concentration[10]

Solution:

$$c(x,t) = c_s\left\{1 - \frac{4}{\pi}\sum_{n=0}^{\infty}\frac{e^{-(2n+1)^2\pi^2 Dt/L^2}}{2n+1}\sin\frac{(2n+1)\pi x}{L}\right\}$$

(19)

Initial Condition:

C(x,0) = C0 for -L < x < L

Boundary Condition:

1. C(-L,t) = Cs
2. C(L,t) = Cs

1.6.1 Typical values of diffusion coefficients in chosen system Cu in Ni, Ni in Cu, Sn in Cu and Ni

1. Cu in Ni: Cu diffusion in Ni-rich solid solutions is studied by means of tracer techniques. The diffusion coefficient at approximately 1000 °C is around 1.0×10^{-16} m²/s.[43]
2. Ni in Cu: Also, diffusion of Ni in Cu-rich alloys at 1000 °C has a diffusion coefficient of 3.0×10^{-17} m²/s, revealing that Ni diffuses more slowly in Cu than Cu would diffuse in Ni.[43]
3. Sn in Cu: Sn diffusion has been measured in the 200–220 °C temperature range in the Cu_3Sn intermetallic phase. Temperature increases the diffusion coefficients, which range from 1.92×10^{-16} to 5.99×10^{-16} m²/s.[44]
4. Sn in Ni: In Ni–Sn diffusion couples, the growth kinetics of intermetallic layers have been used to estimate the diffusion of Sn in Ni_3Sn_4 intermetallic compounds. Approximately 1.0×10^{-16} m²/s is the diffusion coefficient at 175 °C [45].

1.7 Microstructural and Phase Evolution

1.7.1 Cu-Ni System: Microstructural and Phase Evolution

Due to the complete solubility of Cu and Ni in both liquid and solid states, the Cu-Ni system forms a continuous solid solution. The equilibruim phase diagram of Cu-Ni is a simple binary isomorphous system, which exhbits the following characteristcs:

1. A single - phase face-centered cubic (FCC) solid solution at all compositions.
2. There are no intermetallic phases because Cu and Ni have similar atomic sizes and electronegativity.
3. A gradual change in microstructure and mechanical properties depending on the Ni content.

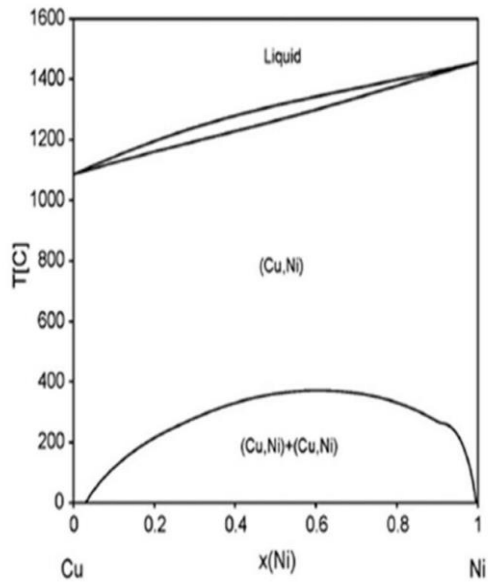

Figure 6 – Phase Diagran of Cu-Ni System [25]

1.7.2 Solidification Behavior of Cu-Ni Alloy

The following microstructural features are present in Cu-Ni alloys during solidification:

1. At low Ni content, the structure resembles pure copper, showing large equiaxed grains.
2. At higher Ni content, solid solution strengthening is noticeable and grain refinement occurs as a result of nickel's influence on nucleation and homogenization treatments improving the uniformity of Ni distribution, and lowering microsegregation.

Mechanical and Physical Properties of Cu-Ni System

1. The alloy have exceptional corrosion resistance, particularly in marine conditions.
2. Hardness and strength increases with Nickel content dur to solid solution strenghtning.
3. The addition of Ni decreases the electrical conductivity, making these alloys suitable for resistivity applications.

1.7.3. Cu-Sn-Ni System: Microstructure and Phase evolution

Phase Diagram and Solidification behaviour: The presence of intermetallic phases makes the Cu-Sn-Ni system more complex than the Cu-Ni binary system. The major features of the phase diagram include:

1. With Cu-rich and Sn-rich phases forming at lower temperatures, Cu-Sn forms an Eutectoid system.
2. The addition of Ni influences the formation of intermetallic compounds such as Ni_3Sn_4 and Cu_6Sn_5.[25]
3. Ni improves the thermal stability of the Sn-rich phases, thereby enhancing the mechanical properties, reducing phase separation and brittle δ-phase.[25]

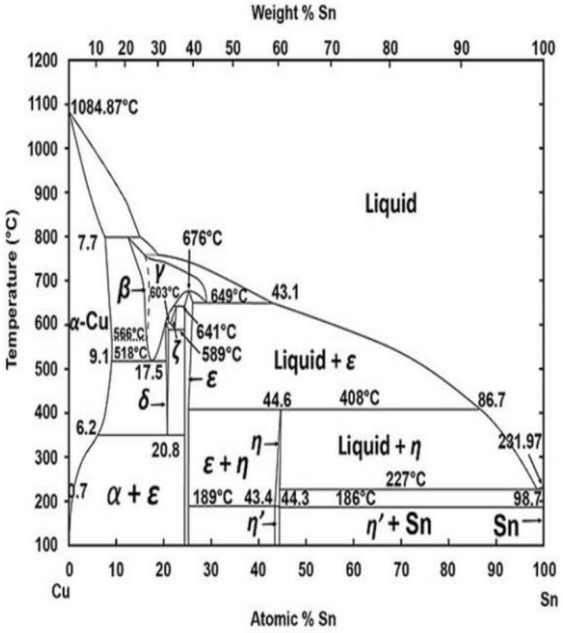

Figure 7 – *Phase* Diagram of Cu-Sn System [25]

Microstructural Evolution during Solidification

1. As-cast Microstructure: At low Ni concentration, □-Cu dendrites form and eutectic structure of (□ + Cu_6Sn_5) appears in the interdendritic areas. At higher Ni content, the grain structure become refined and Ni_3Sn and Cu-Sn-Ni phases are formed.
2. Heat treatment Effects: Heat treatments are applied to improve properties and homogenize the microstructure.
3. Solution Treatment (800-900^{0}C): This treatment dissolves intermetallic phases into the □-matrix, improving ductility.
4. Aging (400-600^{0}C): Ni_3Sn fine particles are precipitated to strengthen the alloy.
5. Annealing (600-750^{0}C): This reduces the internal stresses and enhances wear resistance.

1.7.4 Solidification Behaviour of Cu-Sn-Ni Alloy

I. Nucleation and growth Mechanisms: Composition and cooling rate have impact on the solidification behaviour of Cu-Sn-Ni alloy. These are several key stages:

II. Initial Nucleation: As Ni and Sn decrease the liquidus temperature, the Cu-rich □-phase will be formed, indicating the start of solidification. Additions of nickel promote heterogeneous nucleation at grain boundaries.

III. Primary Dendritic growth: The intermetallic phases (Cu_6Sn_5, Cu_3Sn) or an □-Cu solid solution nucleate and develop as dendrites, depending on the composition. Ni refines dendrite structure, and reducing microsegregation. [25]

IV. Interdendritic Segregation and Eutectic Formation: When the composition is Ni-rich, secondary phases such as Ni_3Sn and Ni_2Sn developed in the interdendritic regions. Slow cooling rate reveals the lamellar eutectic microstructure (□ + Cu_6Sn_5).

V. Post-Solidification Transformations: When the material cools further, some intermetallic compounds precipitate at the grain boundaries. The addition of Ni prevents the formation of the brittle δ-phase via altering the eutectoid reaction.[25]

Property	Cu-Ni System	Cu-Sn-Ni System
Phase Structure	Single-phase FCC Solid Solution	Multi-Phase with intermetallics
Solidification	Continuous Solid Solution	Eutectoid Transformations
Strengthening Mechanism	Solid solution strengthening	Intermetallic Strengthtening
Electrical Conductivity	High	Lower due to intermetallic presence
Wear resisitance	Moderate	High due to Ni_3Sn_4 and Cu_6Sn_5
Application	Used in heat exchangers, desalination systems and maritime components due to their resisitance to corrosion	Used in bearings, bushings, and tribological applications due to their resisitance to wear.

Table 1 – Comparison between Cu-Ni and Cu-Sn-Ni systems

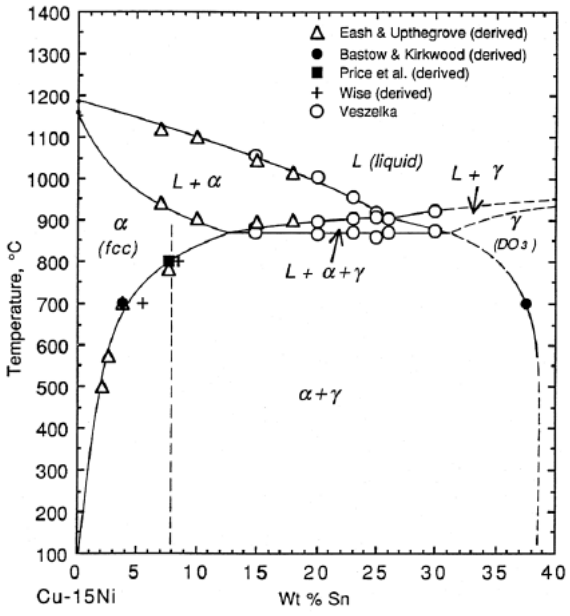

Figure 8 – Cu–Ni–Sn ternary phase diagram

1.7.5 Diffusion Data on Ni-Cu, Cu-Sn, Ni-Sn system.

I Ni–Cu System

1 Grain Boundary Diffusion of Ni in Cu:

Diffusivity (D_{gb}): Measured using radiotracer techniques over 476–1156 K.

Pre-exponential factor (D^0_{gb}): 6.93×10^{-7} m^2/sActivation energy (Q_{gb}): 90.4 kJ/mol [47]

Segregation enthalpy of Ni in Cu grain boundaries: Approximately –17 kJ/mol, indicating moderate segregation tendency

2 Lattice Diffusion of Ni in Cu:

Diffusivity ($D_{lattice}$): $D = 2.64 \times 10^{-7}$ $m^2/s \cdot \exp(-207$ kJ/mol / RT)[48]

Temperature range: 500–650 °C

II Cu–Sn System

1 Grain Boundary Diffusion in Cu–Sn Alloys:

Observation: Addition of 2 wt% Sn to Cu reduces grain boundary diffusion rates for both Cu and Sn.

Activation energy increase: Approximately 0.4 eV compared to pure Cu.

Sn diffusion: Substantially faster along grain boundaries than Cu.[49]

2 Lattice Diffusion of Sn in Cu

Diffusivity ($D_{lattice}$): Values range from 1.92×10^{-16} to 5.99×10^{-16} m^2/s in the Cu_3Sn phase.[50]

Temperature range: 200–220 °C

III Ni–Sn System

1. Grain Boundary Diffusion

Observation: Diffusion-induced grain boundary migration (DIGM) occurs in Ni–Sn alloys.[52]

Mechanism: Sn diffuses along grain boundaries, leading to the formation of alloyed zones and migration of boundaries.

2. Lattice Diffusion of Sn in Ni

Diffusivity ($D_{lattice}$): Approximately 1.0×10^{-16} m^2/s in the Ni_3Sn_4 intermetallic compound.[53]

Temperature: 175 °C

1.7.6 Grain Boundary and Lattice diffusion effects on Cu-Ni and Cu-Sn-Ni Systems

The electrical, thermal and mechanical properties of metallic alloys are mainly influenced by diffusion processes. Cu-Ni and Cu-Sn-Ni alloys undergo two main diffusion mechanisms: bulk diffusion and grain boundary diffusion. [16,17] The interdiffusion kinetics and microstructural evolution of these materials are governed by these mechanisms, which impact their performance in high-temperature applications such as marine components, battery materials and electrical connectors.

1. Lattice Diffusion in Cu-Ni and Cu-Sn-Ni Alloys: Lattice diffusion, also known as bulk diffusion, is the movement of atoms through the crystal lattice of a solid. Its behavior is explained by thermally activated vacancy meditated mechanisms and follows Arrhenius-type behavior. [18]

$$D = D_0 \exp(-Q/RT) \text{ ----------(20)}$$

were,

D is the diffusion coefficient

D_0 is the pre-exponential factor

Q is the activation energy for diffusion

T is the absolute Temperature.

I. Lattice Diffusion in Cu-Ni Alloys

Cu-Ni alloys form a total solid solution since they have identical face-centered cubic (FCC) structure and nearly similar atomic radii (128pm for Cu, 124pm for Ni). The diffusion of Ni in Cu and Cu in Ni occurs via a vacancy exchange mechanism, making lattice diffusion relatively slow compared to grain boundary diffusion.

II. Lattice Diffusion in Cu-Sn-Ni Alloys

Sn atoms in Cu-Sn-Ni systems introduce local strain fields and lattice distortions that affect the diffusion kinetics of Cu and Ni.[18] Unlike the Cu-Ni system's with substitutional diffusion mechanism, the addition of tin influences diffusion in the following ways:

1. By acting as a barrier, preventing the movement of Cu and Ni.
2. By introducing local ordering effects, the diffusion paths are altered.
3. Enhancing the formation of intermetallic phases, which influences diffusion rates.

1.7.7 Grain Boundary Diffusion

Grain boundary diffusion occurs along the interfaces between grains where the atomic packing is less dense than in the bulk lattice. [19] Grain boundary diffusion is significantly much faster than lattice diffusion due to greater concentrations of vacancies at grain boundaries and Lower activation energy for atomic movement.

Grain boundary diffusion coefficient (D_{gb}) is often several orders of magnitude higher than lattice diffusion coefficient (D_L), making it the dominant diffusion mechanism at intermediate temperatures.[19]

$$D_{gb} = D_0^{gb} \exp(-Q_{gb}/RT) \text{ (21)}$$

where,

Q_{gb} is the activation energy for grain boundary diffusion.

Grain Boundary Diffusion in Cu-Ni and Cu-Sn- Ni Alloys

Since Cu and Ni are highly soluble in each other, the role of grain boundary diffusion is reduced in

Cu-Ni alloys compared to lattice diffusion. On the other hand, at temperatures below 800k, grain boundaries becomes more significant in influencing mechanical properties such as creep and fatique resisitance.

When Sn is added to Cu-Ni, grain boundary diffusion becomes a significant process. Sn atoms have the tendency to segregate at grain boundaries, modifying the diffusion behavior of Cu and Ni. This may cause:

1. Higher diffusion occurs on the grain boundaries.
2. The appearance of Sn-rich intermetallic compounds at the grain boundaries.
3. Due to solute drag effect, the movement of grain boundaries is reduced.

1.8 Experimental Techniques for Diffusion Studies

1.8.1 X-ray Diffraction (XRD)

Using XRD, you can learn about the phases and the crystalline structure in an alloy.XRD is the technique employed for the purposes of this study to:

Phase Identification - To detect the appearance of intermetallic compounds or alterations in the crystal structure due to the diffusion of atoms.

Lattice Parameter Studies - To follow even the smallest changes in the lattice constants, as these can indicate the incorporation of alloying elements such as Sn in Cu-Ni.

Evaluating texture and grain size - To check whether diffusion annealing brings changes in crystal orientation or grain growth.

Principles of X-ray Diffraction

X-ray diffraction occurs when there is an interaction of x-rays with the periodic array of atoms in a crystalline material. [20]The periodic arrangement leads to constructive interefernce at specific angles, resulting in a diffraction pattern. The fundamental principle governing XRD is Bragg's Law, which is mathematically expressed as:

nl = 2dsinq---------- (22)

where n is the diffraction order (an integer);

l is the wavelength of the x-rays ;

39

d is the spacing between atomic planes in the crystal;

q is half the scattering angle 2q.

d is the spacing between atomic planes in the crystal

According to Bragg's law, constructive interference occurs when the difference in path length between scattererd x-rays is an integer multiple of the wavelength of the x-ray (Fig 9). At this specific scattering angle 2□□□a diffraction peak is observed in this case. By varying the scattering angle the so-called diffraction pattern is recorded. By analysing it and measuring the spacing between lattice planes, the crystal structure of the material can be determined.

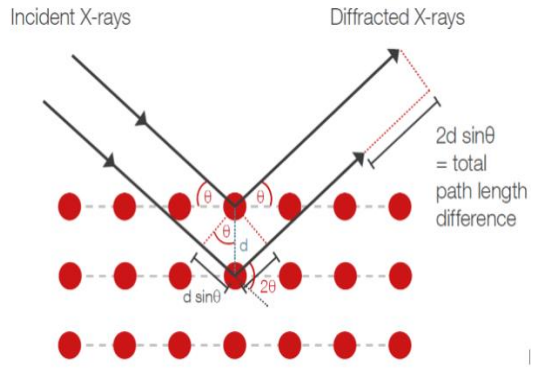

Figure 9 – Diagram of visual representation of Bragg's law. [20]

1.8.2 Scanning Electron Microscopy (SEM) with Energy dispersive Spectroscopy (EDS)

SEM offers a high-resolution imaging of microstructures, while EDS attached to the SEM enables elemental analysis. [21, 22] These techniques are critical for:

1. Microstructural Observation - To visualize the morphology of the diffusion interface and the presence of intermetallic phases.
2. Elemental Mapping - Quantitatively mapping the spatial distribution of Cu, Ni and Sn aross the diffusion couple.
3. Phase Boundary Identification - To Distinquish between regions of solid solution and areas where phase transformations have occurred.

The Basic Principle of SEM

SEM technology operates on the principle of impinging the fine beam of high-energy electrons on the surface of the specimen and obtaining a variety of signals from the specimen surface to determine its properties. When focused on the surface of the specimen, the accelerated electrons in SEM carrying a large amount of kinetic energy. [21] A variety of signals are dissipated when the energy strikes the surface due to the interaction between the electron and the specimen.

The combination of signals includes secondary electrons, backscattered electrons, diffracted backscattered electrons, photons, visible light and heat. These signals are used to determine different information about the specimen surface and in the case of SEM, the secondary electrons, and backscattered electrons are mostly used in producing the image of the specimens. Secondary electrons mainly produce the morphology and topographical information while the backscattered electrons are used to determine the contrasts in the composition of multiphase samples [21].

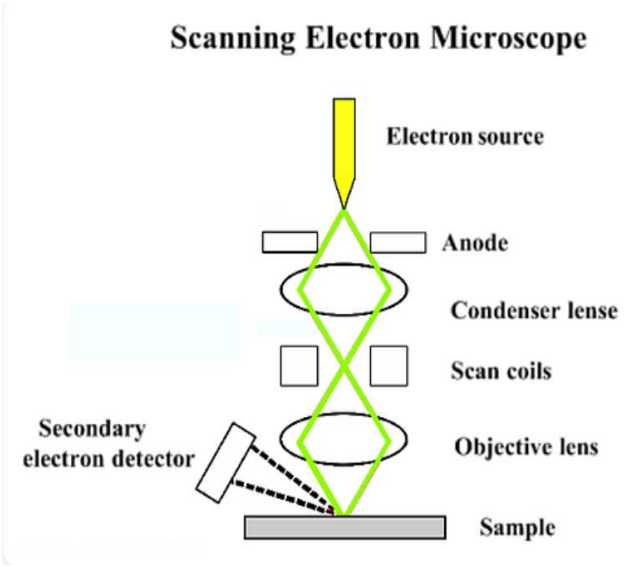

Figure 10 – Showing schematic image of SEM working principle[21]

1.8.3 Wavelength Dispersive Spectroscopy (WDS)

WDS provides a higher spectral resolution compared to EDS, which is particularly useful for:

1. Trace Element Analysis - Identifying minor

variations in composition that are crirtcal when studying interdiffusion in complex systems like Cu-Sn-Ni.

2. Quantitative Analysis - To achieve a more accurate measurements of element concentration at the diffusion interface.

3. Phase Identification - Distinquishing between closely spaced elemental peaks in the spectrum, aiding in the identification of subtle phase changes.

Principles of WDS

When the electron beam in the SEM hits the surface of a sample, it causes the atoms in the material to become excited when they absorbed the energy from the electron beam. When these atoms relax back to their normal state, they released energy in the form of x-rays. The x-rays that are emitted have an energy specific to the element that emitted them.

WDS works on the principle of diffraction. [23] When the x-rays being emitted from the sample enter the WDS, they hit a crystal with specific crystal lattice parameters. This causes the x-rays to diffract (bend), and the amount of the x-rays bend depends on their energy. Thus, the diffractor acts like a prism, separating x-rays by their color (energy), which then travel on to the detector. The instrument has multiple diffractors to cover the entire energy range of interest.

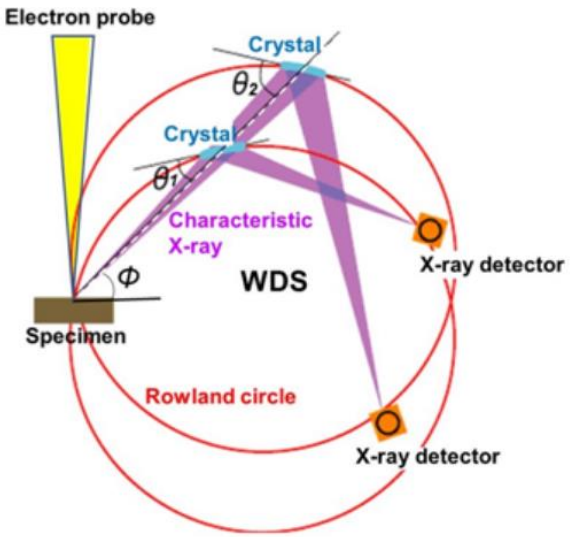

Figure 11 – Showing principles of WDS [23]

1.8.4 Electron Probe Microanalysis (EPMA)

Quantitative chemical analysis and electron microscopy are combined in EPMA to provide:

1. High spatial Resolution - Diffusion profiles are mapped at sub-microns scales.
2. Quantitative Compositional Analysis - Concentration gradients across diffusion interfaces can be precisely determined.
3. Correlation with Microstructure - Integrating compositional data with microstructural features (such as grain boundaries, intermetallic layers).

Principles of EPMA

EPMA operates under the principle that if a solid material is bombarded by an accelerated and focused electron beam, the incident electron beam has sufficient energy to liberate both matter and energy from the sample. [24] These electron-smple interactions mainly liberate heat, but they also yield both derivative electrons and x-rays. Of most common interest in the analysis of materials are secondary and back-scattered electrons, which are useful for imaging a surface and obtaining an average omposition of the

material. X-ray generation is produced by inelastic collision of the incident electrons with electrons in the inner shells of atoms in the sample. When an inner shell electron is ejected from its orbit, leaving a vacancy, a higher shell electro falls into the vacancy and shed some energy as x-rays. [24] These quantized x-rays are characteristics of the element. EPMA analysis is considered to be "non-destrictive", that is x-rays generated by electron interactions do not lead to volume loss of the same, so it is possible to re-analyze the same materials more than one time.

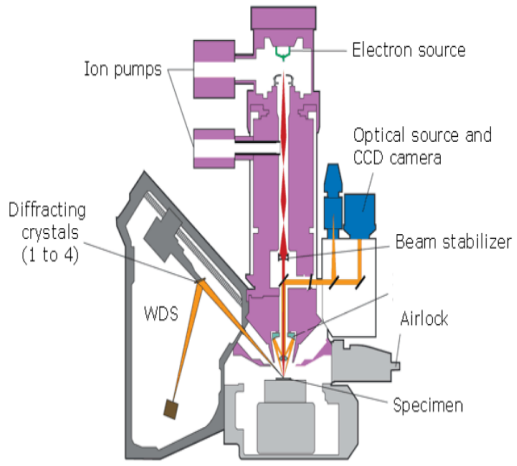

Figure 12 – Diagram of principle of EPMA [24]

1.9 Mathematical and Computational Models for Interdiffusion

In multicomponent alloys, interdiffusion is a complex process by which atoms migrate due to their interactions with temperature, thermodynamics and the concentration gradients. Models and computational approaches give an in-depth understanding of diffusion, but experiments also offer concrete results for diffusion coefficients and interdiffusion profiles. [27]This section explores three key computational approaches:

-Finite Element Modeling (FEM)

-Multi-component Diffusion Simulations

-Machine Learning Techniques for Predictive Analysis.

1.9.1 Finite Element Modeling (FEM) of Diffusion Kinetics

Finite Element Modeling (FEM) is a numerical technique used to solve differential equation related to diffusion by discretizing the problem into small elements and is used in diffusion studies to model phase transformation, diffusion across interface, and time-dependent concentration profiles.

Mathematical Formulation:

Fick's Second law governs interdiffusion in binary and ternary systems.[28]

$$\partial C_i/\partial t = \tilde{N}. (D_{ij} \tilde{N} C_j) \quad (23)$$

where Ci is concentration of component i;

Dij is interdiffusion coefficient matrix;

Ñ is spatial gradient operator;

t is time.

The equations for multicomponent systems must take into consideration cross-diffusion effects, in which the presence of one element affects the diffusion of another. FEM allows for solving these equations in irregular geometrics and heterogeneous microstructures.

Implementation in Cu-Ni and Cu-Sn-Ni systems

1. Mesh Generation - The alloy is divided into discrete nodes using FEM mesh grides.
2. Boundary Conditions - Diffusion couples with fixed positions of Cu-Ni and Cu-Sn-Ni are subject to either Dirichlet or Neumann boundary conditions
3. Time Stepping - The diffusion process is simulated over annealing durations e.g 900k for

Cu-Ni and 750k for Cu-Sn-Ni.

4. Post-Processing- Diffusion profiles and interfacial movement are extracted from FEM simulation.

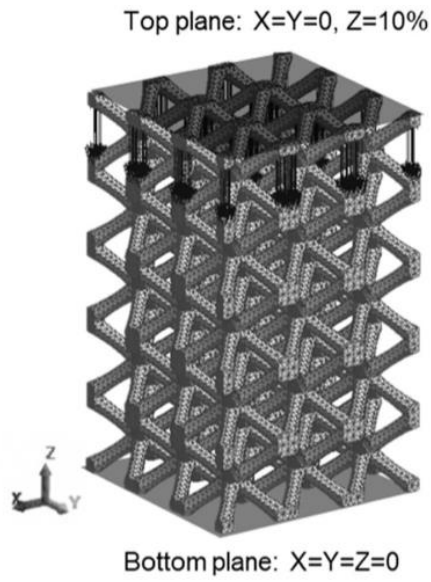

Figure 13 – An example of FEM Model (BCC lattice model) showing boundary conditions[29]

1.9.2 Multi-component Diffusion Simulation Software

Multi-component diffusion software handles numerous elements and uses calculating methods to solve complex diffusion problems, hence providing solutions for interdiffusion problems.

Key software products:

1. DICTRA (Diffusion-controlled Transformation Analysis) is used for:

-The method relies on the CALPHAD technique for analyzing phase diagrams.

-Mobility databases are used to model diffusion kinetics.

-Presents diffusion profiles and predicts when phase transitions will take place.

2. MATLAB and Python for Diffusion Modelling

-Used to develop custom numerical solvers for Fick's laws in ternary systems

-You can use finite difference and volume approaches to solve diffusion equations in MATLAB's PDE toolbox and SCipy in python.

Application to Cu-Ni and Cu-Sn-Ni Systems

1. Cu-Ni - DICTRA predict the effect of Ni concentration on diffusion rate at 900k.

2. Cu-Sn-Ni - Diffusion modeling using CALPHAD helps in understanding the thermodynamic relations between Cu, Sn and Ni.

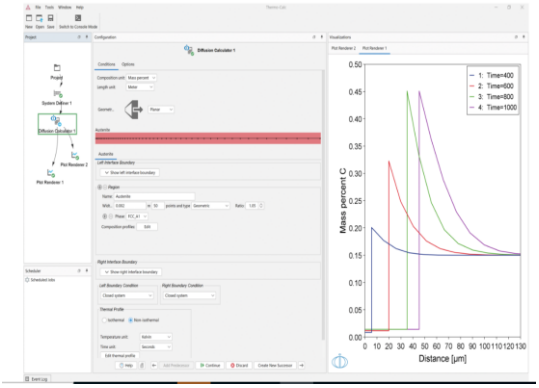

Figure 14 – A screen shot of the diffusion module (DICTRA) showing the results of a moving phase boundary calculation[30].

1.9.3 Machine learning Approaches for Predicting Modeling

Machine Learning (ML) techniques provide a data-driven approach to predict interdiffusion behavior by learning from experimental and simulated datasets. These techniques support the process of learning.

- Identify trends in diffusion coefficient.
- Predict interdiffusion behavior in unexplored temperature-composition ranges.
- Optimize the composition of the alloy to boost control over diffusion.

The Key Machine Learning ML Algorithms include:

1. Artificial Neural Network (ANN)

- Can model nonlinear relationships in diffusion kinetics

- Predicts interdiffusion coefficients for compositions not yet experimentally tested.

2. Gaussian Process Regression or GPR for short

- It allows for making probabilistic estimates of diffusion coefficients.

- Ideal for interpolating diffusion data in situations where experimental datasets are scarce.

3. Support Vector Machines (SVM) for Phase Classification

- Sorts the phases by data collected in experiments and using computer simulations

- Used to approximate the stability of intermetallic compounds at a temperature of 750k

The usefulness of Machine Learning (ML) include:

1. Datasets used are from the Electron Deflection Spectrometry (EDS) and Electron Probe Micro Analyzer (EPMA) for the study of diffusion profiles.

2. Temperature, the chemical composition and the interdiffusion coefficient are treated as input features.

3. Models are built using data from experiments and simulations and they are validated using a process called leave-one-out cross-validation.

4. Using machine learning, the models are able to predict diffusion coefficients for different thermal conditions

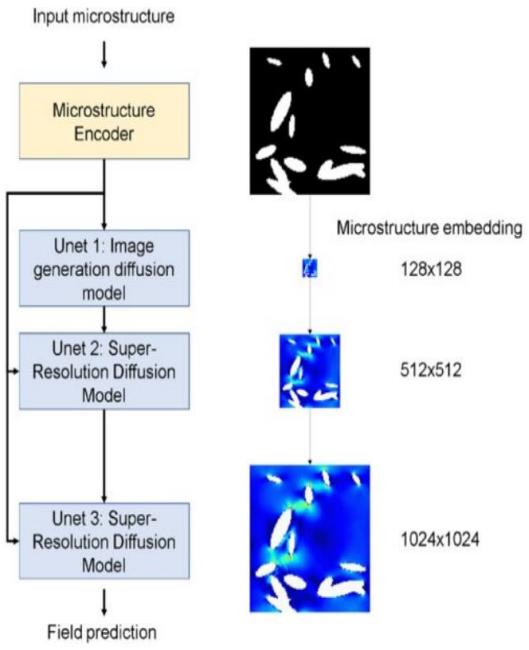

Figure 15 – Summary of the Neural Network architecture of a diffusion based generative model.[31]

The study of interdiffusion kinetics in Cu-Ni and Cu-Sn-Ni alloys require the use of mathematical and computational madels. Finite element modeling provides numerical solutions for diffusion equations, Multi-component diffusion simulation tools like DICTRA allow thermodynamic-based predictions, and machine Learning enables data-driven forecasting of interdiffusion behaviour. By merging both methodologies, this study strenghtens the prediction capacities of interdiffusion studies, delivering useful insights for material design and industrial applictions.

2 Materials and Methods

For investigation the Cu (99,95%), Ni (99%) and Sn (99,9%) purity was used.

Cu-Sn alloy was prepared by direct dissolution of Sn in Cu. The target concentration was 9 mass. % of Sn. The dissolution was made in Al_2O_3 crucible at the temperature 1200 C in quartz tube under Ar atmosphere with addition of H_2. After

heating up to this temperature the system was hold for two hours and cooled down by evacuating of tube from furnace to air.

Cylindrical sample was taken out from crucible, additionally annealed at 850 C for 6 hs, cut to disc, deformed by pressing for 40 % and annealed again at 850 C for 3 hours.

2.1 Diffusion sample preparation.

To understand the most efficient technique, multiple ways were used to to prepare the sample. Diffusion couples were prepared by using a combination of pressing, electrochemical deposition and diffusion bonding to ensure a well-defined, intimate contact between layers.

2.1.1 Sectioning

Samples are cut into appropriate sizes using a precise saw and plasma arc cutting machine to ensure the cut is smooth and free of burrs. Plasma uses -an ionized gas - to create a high temperature arc that cut the metal. Electricity in the plasma raises the temperature enough to cut through the alloy piece. A constant supply of water helps release heat from the workpiece to prevent it from deforming and it also control the metal debris and sparks.

Figure 16 – Typical Plasma Cutting Machine

2.1.2 Grinding

Progressively work with finer grits ranging from (400, 600, 800, 1200, and 4000) to smoothen the surface further. Turn the sample by 90 degrees between each grit to remove scratches from the previous step. The sample should be rinsed after every grinding step and cleaned with alcohol to remove abrasive particles.

2.1.3 Polishing

Use a polishing cloth moistened with a fine diamond or alumina polishing paste. A circular motion was used while polishing to have a shining mirror finish. Wash the sample with water and scrub it with alcohol following every polishing step to eliminate polishing remnants.

2.1.4 Etching

Etching enables the observation of microstructural features in a material. Grain boundaries and other microstructures in copper can be seen after the specimens have been etched. The etchant is prepared suitable for copper and nickel. Among common etchants are Hydrogen peroxide and Ammonium peroxide.

1. Etching Trials - Trial 1

Solution Composition: 10 ml Hydrogen peroxide and 10 ml Ammonium peroxide for a period of 5 minutes.

Observation - The sample was over-etched, resulting in a structure that was not clear under the microscope.

2. Etching Trials - Trial 2

Solution Composition: 5 ml Hydrogen peroxide and 10 ml Ammonium peroxide for a period of 30 seconds.

Observation - The microstructure was clearer, allowing for better analysis.

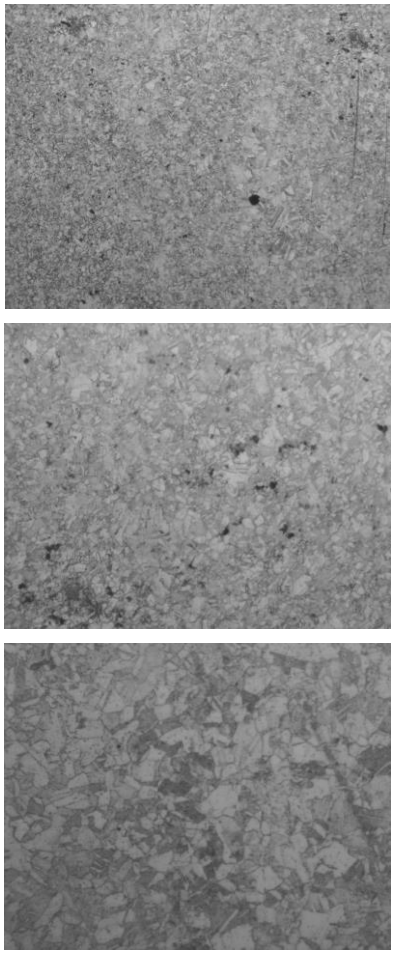

Figure 17 – Microstructural Examination of Cu and Ni ingots after Etching

2.1.5 Annealing of Cu and Ni at 900C

By heating copper-nickel alloys to a set temperature and then cooling them slowly, their microstructure can be modified which improves their strength and toughness. Through this process the internal stresses can be relieved, increase ductility and increase the electrical conductivity of the alloy. The sample is positioned in a furnace. Set the furnace to 900C for annealing the copper-nickel sample. Heat the sample gradually up to 900°C so to ensure uniform heating and to avoid thermal shocks that could lead to cracking.

Figure 18 – Annealing process of Cu-Ni ingots at 900^0C

After the 5-hour annealing period, the material is gradually removed from the furnace and allowed to cool until the material reaches room temperature. Clean the annealed sample to

remove any oxidation or scale that may have formed during the heating process. This can be done using mechanical methods (e.g., brushing or grinding) or chemical methods.

2.1.6 Etching After Annealing

1. Trial 1

Solution Composition - 5 ml Hydrogen peroxide and 10 ml Ammonium peroxide for a period of 30 seconds.

Observation - The sample was over-etched, resulting in a structure that was not clear under the microscope.

2. Trial 2

Solution Composition - 5 ml Hydrogen peroxide, 10 ml Ammonium peroxide and 10 ml Distilled water for 30 seconds.

Observation - The microstructure was clearer, allowing for better analysis.

Figure 19 – Microstructural Examination of Cu and Ni ingots after Annealing and Etching

2.1.7 Bond Formation

The APVM-904 machines are adjusted to offer the optimal pressure for the materials being bonded. Around 25 Tons of pressure is applied to cause plastic deformation at the interface. When pressure is exerted, the surface oxides are broken down and the clean metal atoms come into contact to develop a strong, metallic bond. We maintain the pressure for about 2-5 minutes to ensure a complete bond. This machine, the APVM-904 press, offers an effective and efficient way to bond metals without using heat. However, Despite meticulous preparation and adherence to established procedures, the machine failed to meet the necessary strength and integrity criteria.

Figure 20 – Typical APVM-904 Press Machine for bond formation

This technique in fig 20 was used before for Ni-Cu couples preparation in our laboratory but with very unstable results. We try to develop it to more comfortable level by long annealing of Ni foil and Cu and Cu-Sn alloy to make it softer.

Unfortunately for three layer structure we could not get any reasonable result and typically the atomic contact was not reached except some small area. It can be connected with deformation strengthening of the layer and huge difference in hardness of the layer during the deformation.

Table 2 – shows the initial and final dimensions of the ingot before and after pressing.

Before Deformation								After Deformation							
Diameter of First Sample			Thickness of First sample	Diameter of Second Sample			Thickness of Second sample	Diameter of First Sample			Thickness of First sample	Diameter of Second Sample			Thickness of Second sample
X1(mm)	X2(mm)	X3(mm)	X(mm)	X1(mm)	X2(mm)	X3(mm)	X(mm)	X1(mm)	X2(mm)	X3(mm)	X(mm)	X1(mm)	X2(mm)	X3(mm)	X(mm)
19.3	19.37	19.5	2.95	23.07	23.17	23.15	3	22.53	22.8	22.6	2.46	26.3	26.6	26.25	2.5

2.1.8 Rolling

For initial laying, thin sheets of Cu, Ni and Sn are mechanically pressed to form a flat surface. A manual rolling machine shown in fig 21 is used to couple the part. Prepared Cu/Ni/Cu-Sn sandwich structures were put under the press with varying load and pressed till the significant plastic flow. This method helps to prepare the Cu/Ni/Cu-Sn sandwich structures before diffusion bonding to enable the materials fit in into the cavity or slot cut into another material (steel) prepared for annealing. This is necessary for obtaining good bonding and even contact between parts during diffusion annealing. A manual rolling machine is used to achieve the correct thickness, flatness of the surface and strength in each part.

Figure 21 – Manual Rolling Machine

Figure 22 – Cu/Ni/Cu-Sn sandwch structures after pressing

2.2 Diffusing Bonding

We apply a process called inlaying, which involves inserting the sample (Cu-Ni and Cu-Sn-Ni) into the cavity or slot cut into another material (steel) and then joining them together through treatment. Diffusion bonding is a solid-state joining process in which two or three materials (Cu-Ni or Cu-Sn-Ni) are joined together at an elevated temperature and pressure, but below their melting points. This method rely on the diffusion of atoms between the surfaces of the materials being bonded, creating a strong metallurgical bond without the need of melting the materials.

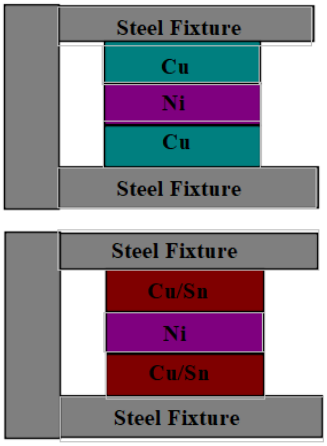

Figure 23a – Schematic illustration of assembly set-up for the Cu-Ni and Cu-Sn-Ni diffusion couples.

Figure 23b – Cu-Ni and Cu-Sn-Ni diffusion couple Assembly Set-up

2.4 Diffusion Annealing

The material is put into a vacuum furnace and heated gradually to 9000°C for the Cu-Ni alloy and 7500°C for the Cu-Sn-Ni alloy. The heating is done gradually to help reduce the thermal stress. It is held at this temperature for 5 hours for the Cu-Ni and 24 hours for the Cu-Sn-Ni system. At this time, Particles from both sides travel to the interface and filling any microscopic voids. The diffusion process improves metallurgical bonding by creating a seamless interface. To stop the metal from oxidizing, annealing is done in a high-vacuum furnace where the air pressure is likely less than 10-5 Torr. After the 5-hour annealing period, the material is gradually removed from the furnace and allowed to cool until the material reaches room temperature.

2.5 Microstructural Investigation

Scanning Electron Microscope (SEM) TESCAN VEGA 3LMH was equipped with an energy-dispersive x-ray spectrometer, X-max 80 (EDS) to examine the microstructure. Distinct grain structures and phase distributions were observed during microstructural examination of both Cu-Ni and Cu-Sn-Ni alloys. Changes in grain size

and distribution due to annealing have a significant impact on the mechanical properties of the materials - hardness, ductility and toughness. Through etchings, you can easily see the grain boundaries and revealing the effects of different processing techniques.

Figure 24 – Scanning Electron Microscopy (SEM)

2.6 Characterization of element distribution after annealing

2.6.1 Energy Dispersive Spectroscopy (EDS)

One essential technique for elemental analysis in material science is energy dispersive spectroscopy (EDS). It is commonly used in combination with scanning electron microscopy (SEM) to ascertain the microscopic composition of materials. EDS is essential to this investigation because it provides both qualitative and quantitative elemental distribution maps across diffusion interfaces, which are used to characterize the interdiffusion process in Cu-Ni and Cu-Sn-Ni systems.This section describes the materials, experimental design, and EDS analytical methodology used to ascertain compositional gradients, intermetallic phase development, and diffusion kinetics.

Materials used in this study for the Cu-Ni diffusion couple is pure Cu and Ni (99.9%) with annealing Temperature 900^0C for 5 hours to study interdiffusion in a completely miscible system and determine diffusion coefficients.

For Cu-Sn-Ni diffusion couple, the materials used include Cu-7.7 wt% Sn alloy and pure Ni (99.9%) with annealing Temperature of 750^0C to study interdiffusion behavior in a system containing a third element (Sn) and assess phase formation at the interface.

High-Temperature Tube Furnace is used for annealing the samples under controlled atmospheric conditions. The furance contains Argon Gas used to prevent oxidation during annealing. After annealing, the samples are mechanically polished using sequentially finer abrasives (Typically 800 (22□m), 1200 (15□m), 2500 (8□m), and 4000 (5□m grits) and finally, samples were fine polished in a 20% water solution of a colloidal silica-based suspensions to remove surface oxides and achieve a mirrior-like finish.

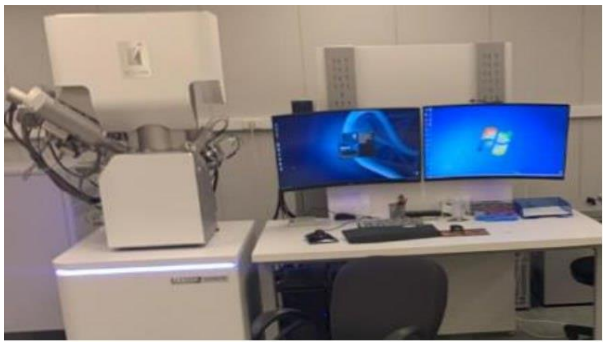

Figure 25 – Typical Energy Dispersive Spectroscopy (EDS)

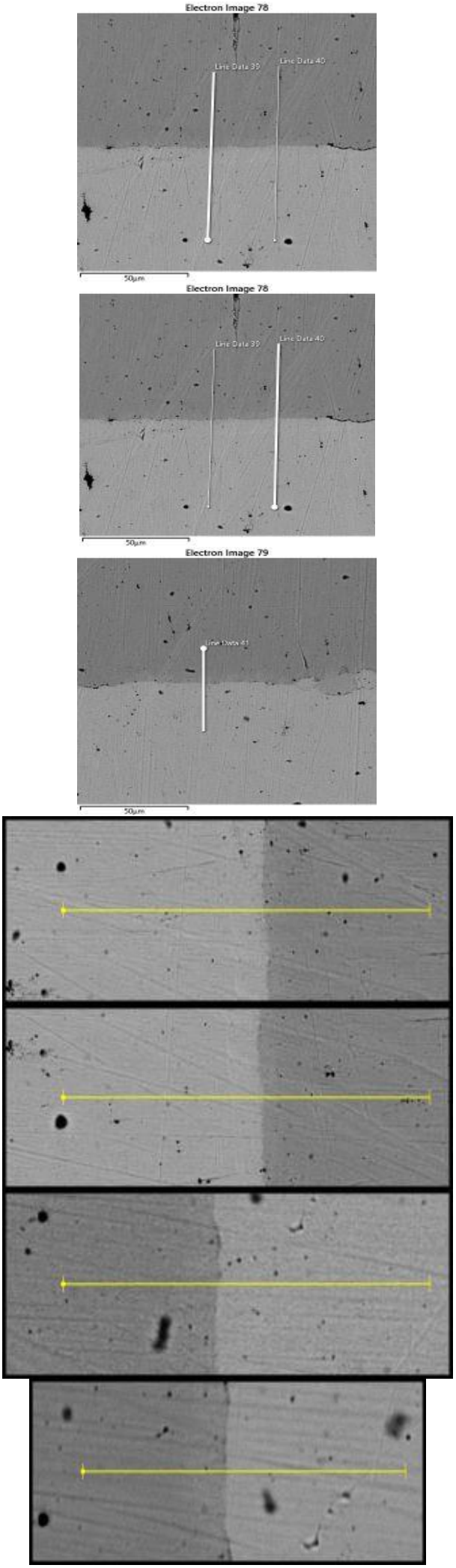

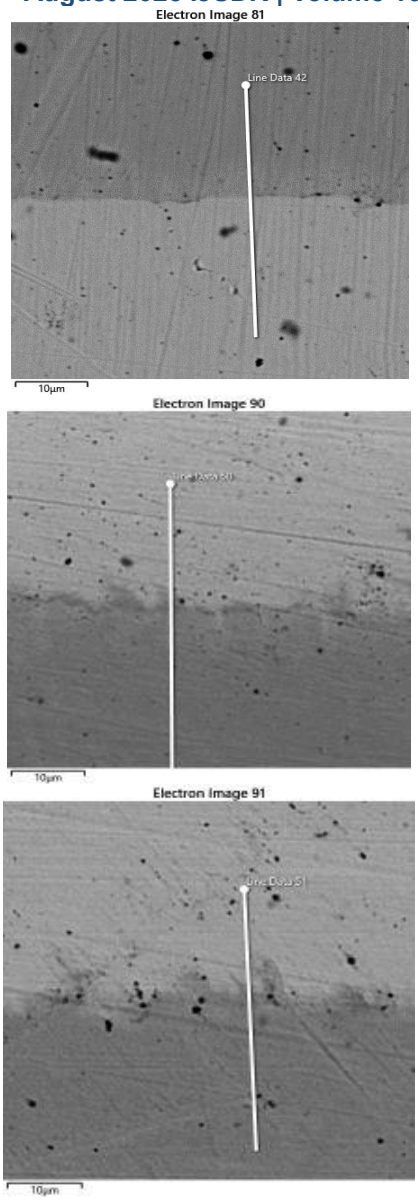

Figure 26a – EDS Elemental Line Mapping for Cu-Ni diffusion couple

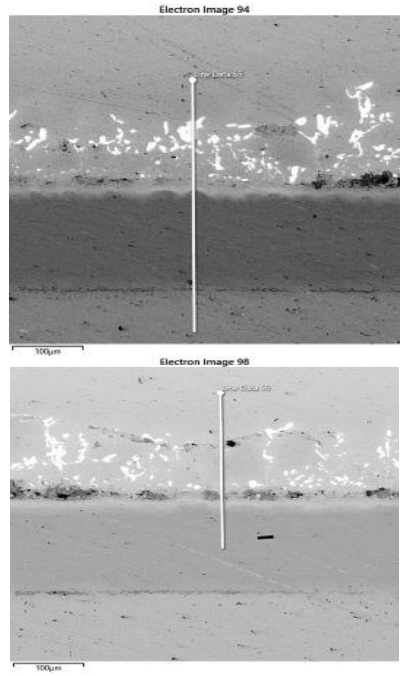

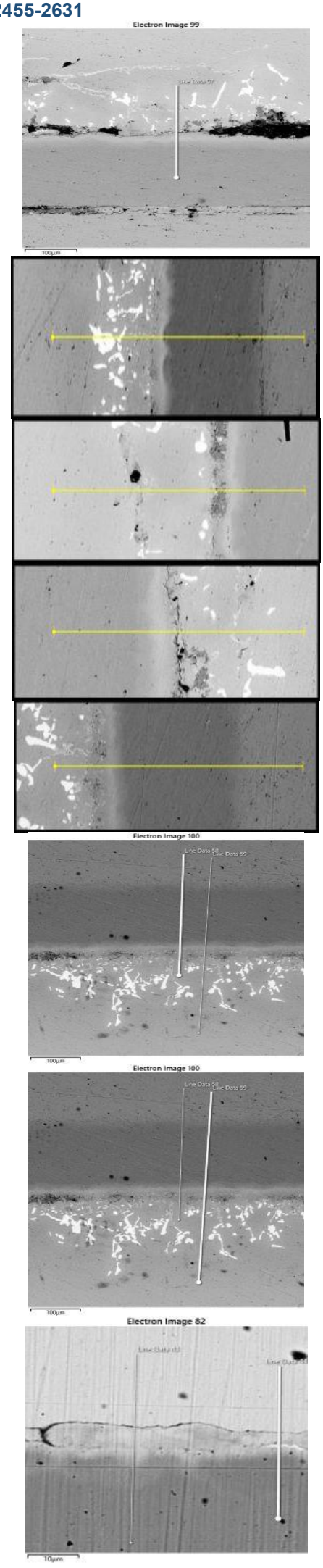

Figure 26b – EDS Elemental Line Mapping for Cu-Sn-Ni diffusion couple

3 Results and Discussion

Fig 2 shows the SEM micrographs from the interface of the Cu-Ni and Cu-Sn-Ni diffusion couples annealed at temperatures 900^0C and 750^0C for 5 and 24 hours respectively. The micrographs showed an approximate and perfect physical contant between Cu-Ni and Cu-Sn-Ni sheets at interfacial zone as a primary important factor for the diffusion and formation of intermetallic compounds. In the majority of the formed interfacial compounds, near-straight intermetallic layers can be seen with minor uneven interface which would be related to the probable non-uniform distribution of pressure applied to the Cu-Ni and Cu-Sn-Ni interface.

Two intermetallic phases of Cu_6Sn_5 and Ni_3Sn_4 are clearly present in these specimens, regardless of the Ni content in the Cu-Sn-Ni alloy, as indicated in (fig 2). The quantitative results are represented in Table 3.

3.1 Phase Identification of Cu-Sn-Ni Diffusion System

In the Cu–Sn–Ni system, diffusion results in the formation of several solid solution zones and intermetallic compounds (IMCs). The phase identity is determined by the elemental composition of the various reaction zone regions. The IMCs generated and their relationship to diffusion paths and phase stability are identified in this investigation using EDS data from three sets of spectra (S1 to S7) from various locations

of the Cu–Sn–Ni interface.

.1.1 Compositional Data Summary and Phase Identification

Table 3(a - i) – The Chemical Composition of different IMC phases at different locations analyzed by EDS (At%)

Spectrum	Composition (at%)			Phase Interpretation
	Ni	Cu	Sn	
S 1		93.65	6.35	Ni-rich solid solution(Ni-Cu alloy)
S 2	100			Pure Ni
S 3		100		Pure Cu

Table 3a - repesent base metals: Ni-rich alloy (S1) pure Ni (S2), and pure Cu (S3)

Spectrum	Composition (at%)						Phase Interpretation
	Cr	Fe	Ni	Cu	Mo	Sn	
S 1			100				Pure Ni
S 2	0.77	3.47	43.2	51.14	1.15	0.28	Cu-Ni solid solution with Fe, Cr as impurities
S 3	0.3	1.18	70.8	27.19	0.29	0.21	Ni-rich alloy with minor Sn
S 4				100			Pure Cu
S 5	0.37	1.45	34.1	63.29	0.35	0.46	Cu-Ni solid solution with Fe, Cr as impurities

Table 3b Spectrum (S3-S5) lie in a solid solution region ahead of intermetallic formation (Sn is low, thus no defined IMC is formed. These are transitional regions between Cu and Ni.

Spectrum	Composition (at%)			Phase Interpretation
	Ni	Cu	Sn	
S 1	0.48	92.98	6.54	α-Cu solid solution with Sn
S 2	98.38	1.62		Pure Ni
S 3	86.78	4.16	9.06	Ni-rich ternary IMC(possibly Ni_3Sn_4)
S 4	90.63	3.54	5.83	Ni-Sn IMC

Table 3c Spectrum 1 represents Cu-rich region with dissolved Sn likely near the Cu base, spectrum (S3-S4) has high Ni content with increasing Sn indicating Ni_3Sn_4 IMC.

Spectrum	Composition (at%)			Phase Interpretation
	Ni	Cu	Sn	
S 1	48.13	48.32	3.55	Cu-Ni Solid Solution
S 2	74.07	7.4	18.5	Ni-rich IMC: Ni_3Sn_4
S 3	62.53	22.6	14.9	Ni-rich IMC

In table 3d, spectrum 1 lies at the boundary of a solid solution, where spectrum (S2-S3) suggest the formation of Ni_3Sn_4 IMC.

Spectrum	Composition (at%)			Phase Interpretation
	Ni	Cu	Sn	
S 1	68.64	9.17	22.2	Ni_3Sn_4
S 2	69.32	8.71	22	Ni_3Sn_4
S 3	63.32	17.94	18.7	$(Cu,Ni)_6Sn_5$
S 4	90.42	4.93	4.65	Ni solid solution
S 5	1.66	92.5	5.84	Cu solid solution

Table 3e the Spectrum (S1-S2) shows clear evidence of Ni_3Sn_4 and Spectrum S3 suggested the possibility of $(Cu,Ni)_6Sn_5$ IMC.

Spectrum	Composition (at%)			Phase Interpretation
	Ni	Cu	Sn	
S 1	1.24	93.01	5.75	α-Cu solid solution
S 2	1.07	92.98	5.95	α-Cu solid solution
S 3	85.56	7.08	7.36	Ni-rich ternary IMC
S 4	96.24	2.8	0.96	Ni solid solution with slight Sn
S 5	84.41	8.64	6.95	$(Cu,Ni)_6Sn_5$ IMC

In table 3f, the Spectrum(S1-S2) clearly show Cu solid solution zone while Spectrum (S3-S5) are part of the Ni-rich reaction front where IMC form.

Spectrum	Composition (at%)			Phase Interpretation
	Ni	Cu	Sn	
S 1	41.44	33.45	25.11	likely $(Cu,Ni)_6Sn_5$-ternary Ƞ-phase
S 2	42.05	32.67	25.28	likely $(Cu,Ni)_6Sn_5$-ternary Ƞ-phase
S 3	42.58	33	24.43	likely $(Cu,Ni)_6Sn_5$
S 4	10.23	86.24	3.53	Cu-rich solid solution(α-Cu with Ni, Sn)
S 5	7.06	89.87	3.07	α-Cu solid solution-slight diffusion of Sn, Ni

In Table 3g, Spectrum (S1-S3) compositions are very close to the known ternary compound $(Cu,Ni)_6Sn_5$, derived from Cu_6Sn_5 Ƞ-phase substituted by Ni. Spectrum(S4-S5) is within the Cu substrate which represents a Cu-rich region.

From the table 3h, spectrum (S2-S3) are consistent with $(Cu,Ni)_6Sn_5$ IMCs. S1 is a Cu-rich phase near the Cu side while S4-S6 represent the undisturbed Cu which is mainly pure Cu region. S7, with high Ni and moderate Sn, points to Ni_3Sn_4, a key Ni-Sn intermetallic phase formed on the Ni side of a Cu-Sn-Ni diffusion couple.

Spectrum	Composition (at%)			Phase Interpretation
	Ni	Cu	Sn	
S 1	5.52	90.17	4.31	α-Cu solid solution (with minor Sn and Ni)
S 2	18.12	78.31	3.57	Cu(Ni,Sn) alloy
S 3	1.47	98.53		pure Cu
S 4	0.79	99.21		pure Cu
S 5	0.48	99.52		pure Cu
S 6	82.88	17.12		Ni-rich phase(possibly Ni-Cu solid solution)

In table 3i, Spectrum (S1-S2) located near the intermetallic front represent the transitioning from Cu-rich region to solid solution or pre-IMC zone. S6 is pure Ni region and no Sn detected possibly due to limited penetration.

3.2 Microstructural Analysis of Cu-Sn-Ni Diffusion System

The EDS analysis confirms that the Cu-Ni binary samples predominantly consist of pure Cu region, Pure Ni regions, Cu-Ni solid solutions and no intermetallic compounds due to full solubility at

Spectrum	Composition (at%)			Phase Interpretation
	Ni	Cu	Sn	
S 1	3.82	92.99	3.19	α-Cu solid solution
S 2	41.99	33.14	24.86	$(Cu,Ni)_6Sn_5$ IMC
S 3	44.69	30.69	24.62	$(Cu,Ni)_6Sn_5$ IMC
S 4	91.26	8.74		Pure Cu
S 5	0.85	99.15		Pure Cu
S 6	0.93	99.07		Pure Cu
S 7	72.83	22.69	4.48	Ni_3Sn_4 or Ni rich ternary $(Ni,Cu)_3Sn_4$

elevated temperatures (FCC solid solution). The Cu-Ni system forms a continuous solid solution based on the FCC lattice structure. Thus the observed microstructures are homogeneous solid solutions with slight variations in compositions. There is a single-phase FCC grains (α-Cu) throughout the microstructure due to complete solid solution. (fig. 27).

The observed microstructures are uniformity under SEM due to solid solution. No sharp phase boundaries are formed and the smooth EDS compositional gradients forms a substituional solid soluton. There is a gradual compositional transition betweeen Cu and Ni rather than sharp interfaces due to low atomic contrast between grains. The presence of pure Cu and pure Ni regions indicates limited interdiffusion at the extreme sides. Near the Matano interfaces, we observed equiatomic Cu-Ni solid solution, (fig 28) which is consistent with a continuous interdiffusion front. It can also be observed that the formation of a fine morphology close to the

Cu side indicates faster diffusion rate of Ni element towards Cu, leading to saturation of Ni in the Cu solid solution.

The microstructural features indicate a multiphase structure with bright and dark regions under SEM micrographs in figure 27. The bright regions have a higher atomic number (Ni_3Sn_4, and Cu_6Sn_5 intermetallic compounds) while the dark regions are Cu-rich a-solid solution. There is a sharp interfaces between intermetallics and solid solutions resulting that the phase boundaries in Cu-Sn-Ni system are sharper than the Cu-Ni system. The addition of Sn facilitates the formation of intermetallic phases. Ni_3Sn_4 phase forms fine, discrete particle or layered precipitates and grow slowly due to limited diffusivity of Sn in Ni. There is an increase in hardness and brittleness of Cu-Sn-Ni system due to the formation of intermetallic compounds compared to the Cu-Ni binary system. It is of Note that before the exhaustion of Sn in Cu-Sn-Ni, the dominant reaction is the growth of Cu6Sn5 at the expense of Cu and Sn ie

$$6Cu + 5Sn = Cu_6Sn_5 \text{----------(24)}$$

The presence of Ni in Cu_6Sn_5 can be ignored in Eq (1) due to the fact that most Cu_6Sn_5 have relatively small amounts of Ni. The Cu diffusivity and Sn diffusivity in Cu_6Sn_5 are comparable, [34], and consequently both Cu and Sn atoms diffuse through the Cu_6Sn_5 layer to react with other elements to form Cu_6Sn_5.

In the Cu-Ni-Sn ternary systems, the presence of Cu can slightly shift the phase boundaries generally supporting the formation of Ni_3Sn_4 as a result of Cu's limited solubility in Ni_3Sn_4 and Cu's suppression of other intermetallic compounds due to competitive reactions.

The formation of Ni_3Sn_4 generally proceeds through a solid-state diffusion reaction between Sn-rich layers and Ni substrates, often facilitated by the Kirkendall effect and vacancy migration. Here, Ni acts as the dominant diffusing species and Sn originates at the interface with Cu/Ni layer. The dominant reaction at this stage can be written as:

$$3Ni + 4Sn = Ni_3Sn_4$$

(25)

In layered diffussion couples, Ni diffuses toward Sn, reacting at the interface to form Ni_3Sn_4. The growth follows a parabolic time law, indicating diffusion controlled growth. It is of note that Ni_3Sn_4 growth rate is typically faster than that of Cu_6Sn_5 due to the high diffusion rate of Sn in Ni. In addition of Cu suppresses the formation of Ni_3Sn_4 because it forms other intermetallic compounds that may compete for Sn. This behaviour was observed in table 3 where compositions such as Ni□□ 63%, Cu □ 17.9% and Sn □ 18.7% suggesting that Cu is partially incorporating into Ni_3Sn_4 lattice, forming a Cu-Sn-Ni solid solution phase structurally similar to Ni_3Sn_4.

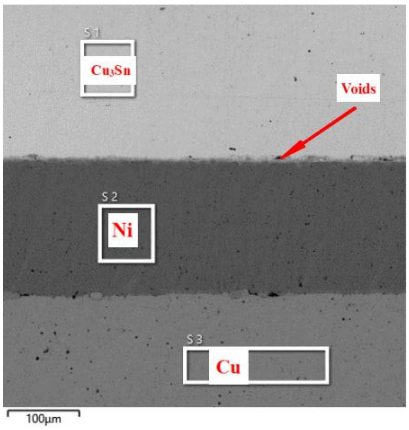

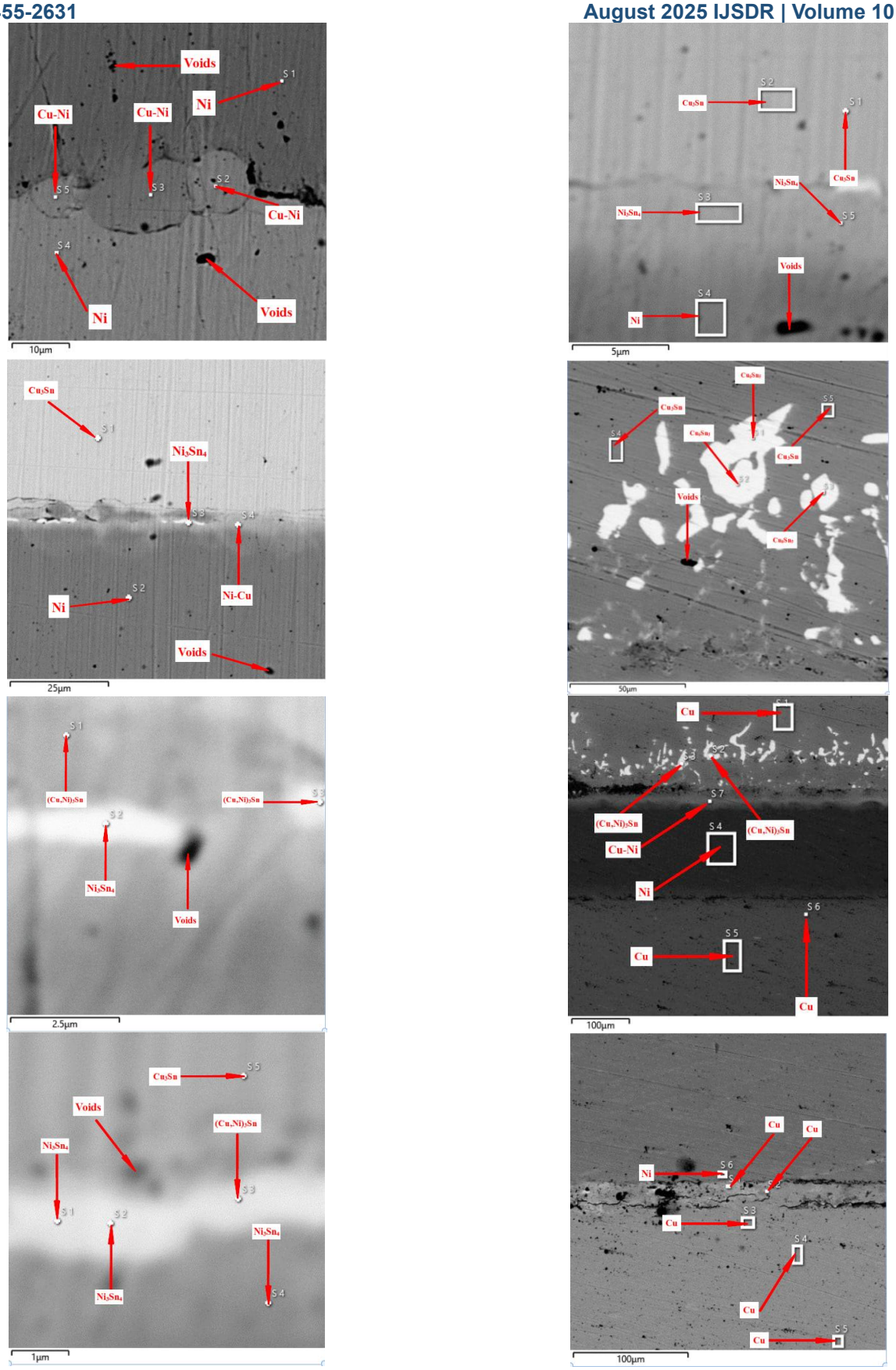

Figure 27 – SEM Micrographs from the cross-section of Cu-Ni and Cu-Sn-Ni Interfaces annealed at 900^0C and 750^0C for 5 hours and 24 hours

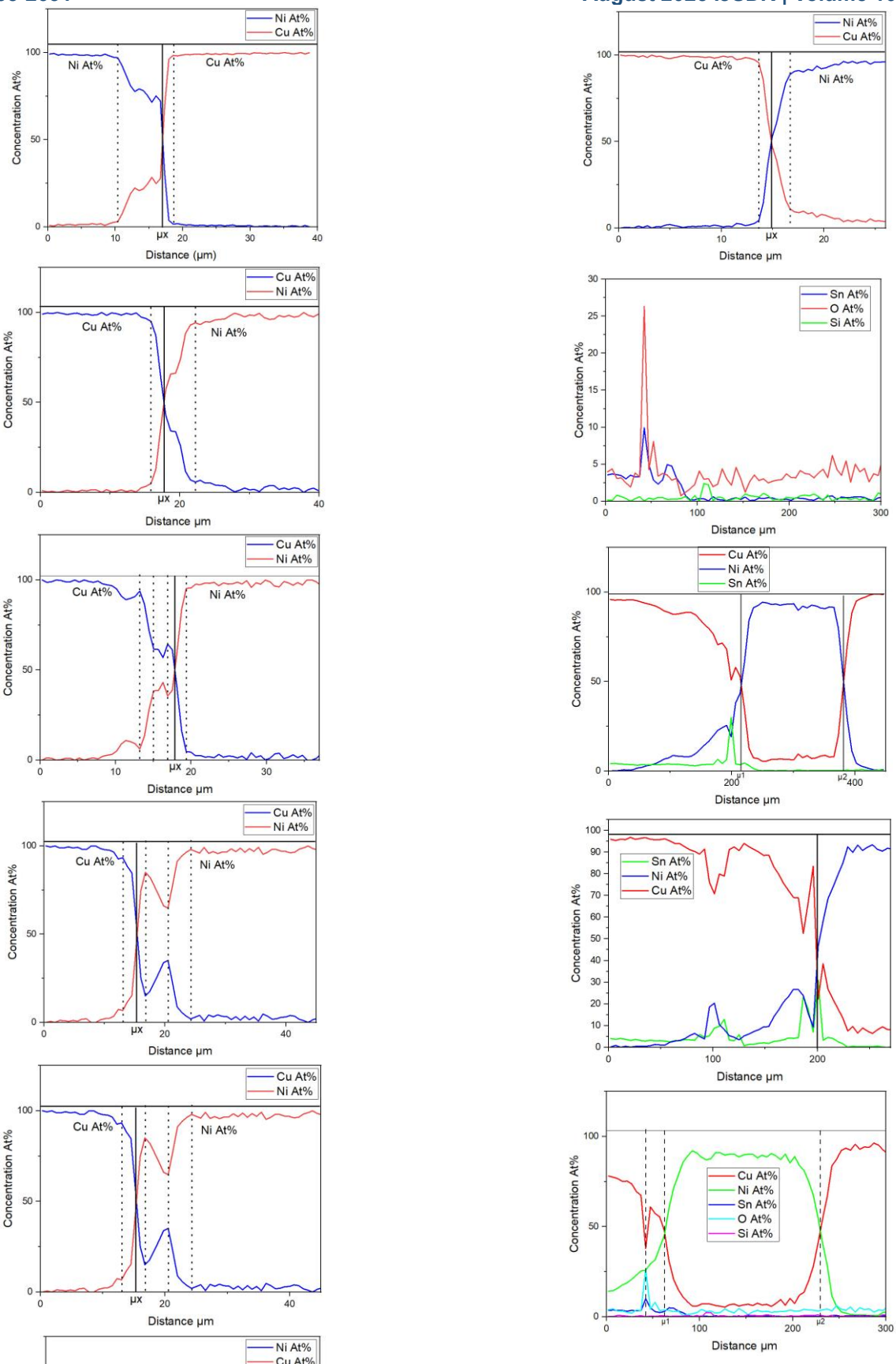

Figure 28 – EDS Line Scan analysis results for the cross sections of Cu-Ni and Cu-Sn-Ni interfaces annealed at 900^0c and 750^0C for 5 and 24 hours

3.3 Calculation of Diffusion Coefficients

As one can see the processes at two interfaces can be described separately because the thickness of Ni foil is sufficiently large. At the interface Cu/Ni the interdiffusion coefficient in Cu-Ni can be used to describe the diffusion. It is known that interdiffusion coefficient depends on concentration. One can see only slight asymmetry of profile so we use approximation that profile can be describe by two erf-like functions with two diffusion values of diffusion coefficients: $C = A + Berf\left\{\frac{x-x_0}{A}\right\}$ (26)

where, $A = 2\sqrt{(Dt)}$

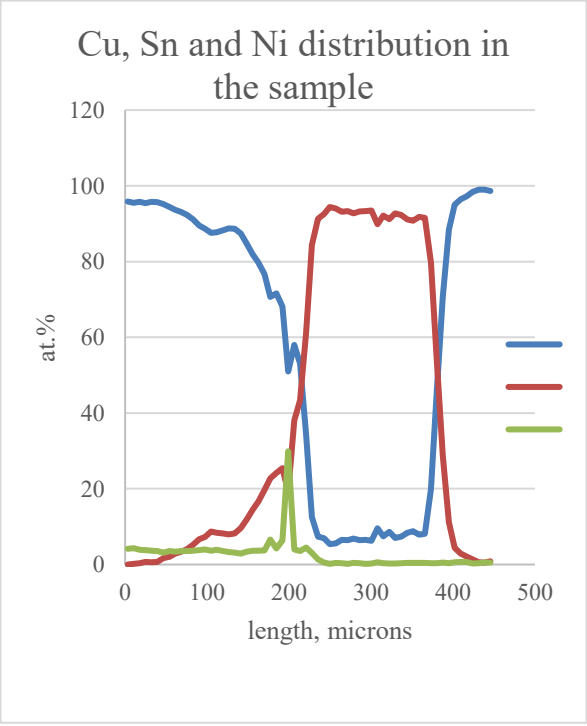

Figure 29 – Elemental Distribution Profile of Cu, Sn, and Ni Across the Cu–Sn/Ni Diffusion Couple

For Ni rich zone A is 12 μm, and for Cu rich A is 17 μm. At the interface Cu-Sn/Ni the main processes are redistribution of Cu and Sn. As it was mentioned Sn flux directed to the zone of formation of intermetallics while Cu flux directed to into the Ni. Strong asymmetry of Cu profile can be seen (the profile is presented at figure 30). In Ni zone Diffusion coefficient is 4.17E-16 $\mu m^2/s$ while in In Cu zone, Diffusion coefficient is 8.36E-16 $\mu m^2/s$. The implication is that Cu diffuses twice as fast as Ni into the system in their respective rich zones. This implies that Cu atoms penetrate deeper into the Ni side than Ni atoms into the Cu side over the same time period. This is consistent with the asymmetry profile observed in the concentration profile as seen in figure 30. The diffusion couple clearly defined the interdiffusion zone with sigmoidal concentration profiles as a result of binary metallic diffusion.

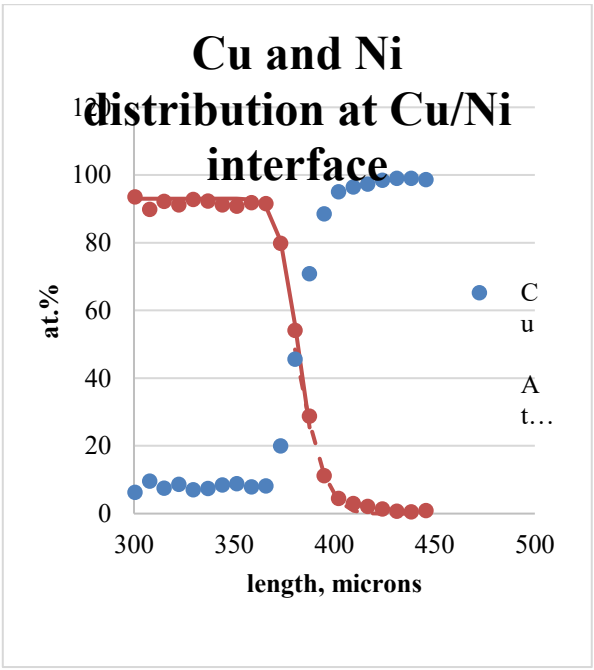

Figure 30 – Concentration Profile of Cu and Ni Across the Cu/Ni Interface after Diffusion

Diffusion coefficient of Cu–Sn rich zone is 8.36E-04 $\mu m^2/s$. This value is larger than the diffusion coefficients in the pure Cu–Ni or Ni–Cu zones. This implies that Cu spreads more deeply into the Ni interface than Sn. Sn has a low concentration as a result it shows a measurable profile despite its low concentration. The higher

diffusion coefficient in Cu-Sn suggests greater atomic mobility in Cu–Sn which can be due to higher vacancy concentration, lattice distortion from Sn atom and possibly due to lower activation energy of Sn.

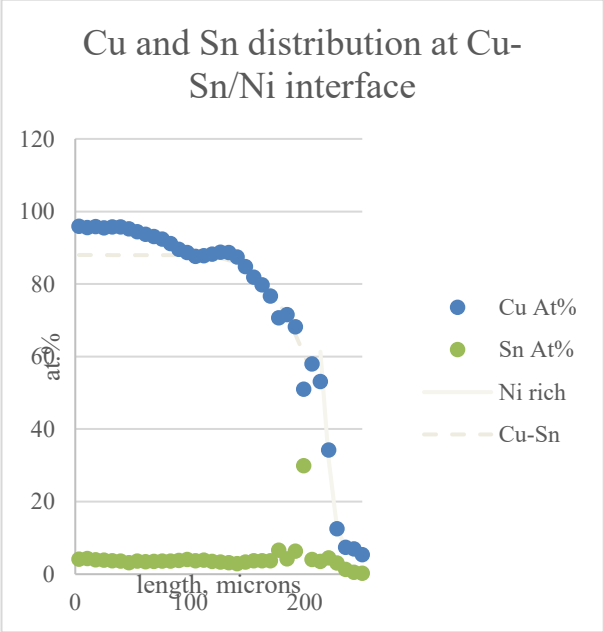

Figure 31 – Elemental Distribution of Cu and Sn Across the Cu–Sn/Ni Interface After Diffusion

Using the same approach the values of A 12 μm and 55 μm can be obtained for Ni and Cu-Sn zone. This values corresponds to the following diffusion coefficients at 750 C

- In Ni zone D = 4.17E-16 m^2/s
- In Cu zone D = 8.36E-16 m^2/s
- In Cu-Sn zone D = 8.75E-15 m^2/s

Interdiffusion coefficient depends on concentration. One can see only slight asymmetry of profile so we use approximation that profile can be described by two erf-like functions with two diffusion values of diffusion coefficients.

According to Paul et al. (2004) and Tu (2002),[37,40] interdiffusion coefficients of Cu-Ni at 900 °C range between **10^{-16} to 10^{-15} m^2/s**, which agrees the values obtained for Ni-rich and Cu-rich zone values.

Diffusion coefficients reported in literature for Cu_3Sn and Cu_6Sn_5 formation lie in the range of **10^{-14} to 10^{-15} m^2/s** at 750–800 °C (Zhou et al., 2015; Laurila et al., 2005), [32] validating the value of Cu-Sn zone result of **8.75×10^{-15} m^2/s**.

CONCLUSION

This research examined the diffusion behaviour, formation of intermetallic compounds and distribution of elements in the systems Cu–Ni and Cu–Sn–Ni when annealed at high temperatures. Outcomes from these experiments are significant for joining materials, metallurgical processing and microelectronic packaging. The main results could be summarized as following:

1. The value of the diffusion coefficient for Cu in the Cu-rich side of the Cu–Ni system is D(Cu in Cu rich zone) is 0.000836 $\mu m^2/s$. In terms of Ni, the Ni-rich region it is = 0.000417$\mu m^2/s$.
2. The Cu–Ni couple was annealed at 900 degrees Celsius for a total of 5 hours. Despite the short duration and high temperature, a great deal of interdiffusion took place which proved that Cu diffuses twice as fast as Ni under these conditions. Asymmetric interdiffusion zone was observed with Cu penetrating deeper into Ni.
3. In the Cu–Sn–Ni system, the diffusion coefficient in the Cu–Sn region was identified as 0.004875 $\mu m^2/s$ annealed at 750°C for a period of 24 hours. This high value suggests that Sn significantly enhances diffusion and facilitating

intermetallic phase growth like $(Cu,Ni)_6Sn_5$ or Ni_3Sn_4.

4. A clear transition from Cu to Ni was seen in the interface, showing that minimal intermetallic compound formed and the interdiffusion zone is characterized by gradual concentration changes. The high mobility of Cu makes mass transport mechanism possible.

5. The Cu-Sn-Ni system demonstrated complex diffusion that caused Sn to accumulate mostly in the interfaces.

6. The presence of intermetallic compounds was identified using compositional peaks and results from EDS spectra.

7. Since the diffusion coefficient is much greater ($D \approx 0.004875$ μm²/s), this suggests that there are more rapid paths for diffusion such as grain boundary diffusion and Reaction diffusion in Sn-rich compounds.

8. The presence of Sn in Cu-Sn led to more pronounced interdiffusion and intermetallic formation. This confirms the critical role of Sn as a diffusion enhancer.

9. In diffusion soldering and transient liquid phase bonding, Sn serves as a diffusional bridge and accelerator, but its amount but must be controlled to avoid formation of brittle intermetallics.

10. Asymmetric diffusion in the Cu–Ni couple influences bimetallic corrosion, joint stability and creating gradient microstructures design.

11. The measured diffusion coefficients support Fickian behavior in binary systems and enhanced, non-linear diffusion in ternary systems.

12. The main outcome is the quantitative confirmation of Sn's catalytic role in diffusion, which should be considered in multi-material interface design.

As proven by this thesis, Cu–Sn–Ni diffusion couples show detailed yet controlled behavior that is significant for solder joints design, metallurgical joining and the development of multi-phase diffusion materials.

REFERENCES

1. Boris S. Bokstein, Mendelev, M. I., & Srolovitz, D.J. (2005) "Thermodynamics and Kinetics in Materials Science", 2nd edition, Oxford University Press, Chapter 10.
2. J.G. Kirkwood. et al. (1960)Flow equations and frames of reference for isothermal diffusion in liquids. The Journal of Chemical Physics 33(5):1505–13.
3. Ehrhart, P. (1991) "Properties and interactions of atomic defects in metals and alloys", chapter 2, p.88 in Landolt-Börnstein, New Series III, Vol. 25, Springer, Berlin.
4. P. Heitjans, J. Karger, Ed, "Diffusion in condensed matter: Methods, Materials, Models," 2nd edition, Birkhauser, 2005, pp. 1-965.
5. Fisher, J. C. (January 1951). "Calculation of Diffusion Penetration Curves for Surface and Grain Boundary Diffusion". Journal of Applied Physics. 22 (1): 74–77.
6. Le Claire AD, Rabinovitch A (1981) Approach to the problem of diffusion in dislocations. J Phys C Solid State Physics 14:3863, 1981
7. Atkins P, de Paula J (2006). Physical Chemistry for the Life Science.
8. Conlisk, A. Terrence (2013). Essentials of Micro- and Nanofluidics. p. 43.

9. Medvedev, O. (2005). Diffusion Coefficients in Multicomponent Mixtures Technical University of Denmark.
10. Boris S. Bokstein, Mendelev, M. I., & Srolovitz, D.J. (2005) “Thermodynamics and Kinetics in Materials Science”, 2nd edition, Oxford University Press, Chapter 10. chapter 10, p.167
11. Philibert J (2005). "One and a Half Centuries of Diffusion: Fick, Einstein, before and beyond" (PDF). Diffusion Fundamentals. 2: 1.1–1.10.
12. Darken, L. S. "Diffusion, mobility and their interrelation through free energy in binary metallic systems". Trans. AIME 175.1 (1948): 184–194.
13. Smigelskas, A. D., and E. O. Kirkendall. "Zinc diffusion in alpha brass".Trans. AIME 171 (1947): 130–142.
14. R. E. Cunningham et al., Diffusion in Gases and Porous Media Springer Science and Business Media New York 1980.
15. Helmut Mehrer, Nicolaas A. Stolwijk. “Heroes and Highlights in the History of Diffusion”. diffusion-fundamentals.org 11 (2009) 1, pp 1-32
16. Mehrer, H. (2007). Diffusion in solids: Fundamentals, Methods, Materials, Diffusion-controlled processes. Springer
17. Campbell, F.C. (2008). Elements of Metallurgy and Engineering Alloys. ASM International.
18. Glicksman, M.E. (2000). Diffusion in Solids: Field Theory, Solid-State Principles, and Applications. Wiley.
19. Mishin, Y., & Herzig, C. (2000). Grain Boundary Diffusion, Stresses, and Segregation in Alloys. Springer.
20. Harold P. Klug and Leroy E. Alexander, “X-ray Diffraction Procedures: For Polycrystalline and Amorphous”.
21. Joseph Goldstein et al “Scanning Electron Microscopy and X-ray Microanalysis”
22. Yang Leng. ”Materials Characterization: Introduction to Microscopic and Spectroscopic Methods”.
23. T.M. Clegg, “Wavelength Dispersive X-ray Spectrometry: A practical Guide”.
24. R.C. Price, “Electron Probe Microanalysis and Scanning Electron Microscopy in Geology”.
25. Andreas Leineweber, “The Cu–Sn System: A Comprehensive Review of the Crystal Structures of its Stable and Metastable Phases” J. Phase Equilib. Diffus. (2023) 44:343–393
26. Guo, L.; Zuo, P.; Zhang, Z.; Zhang, Q.; Zhao, M.; Hou, X.;Wu, J.; Zhang, B. A Review of Cu–Ni–Sn Alloys: Processing, Microstructure, Properties, and Developing Trends. Materials 2023, 16, 444.
27. Robert Filipek, “Mathematical model of interdiffusion in multi-component open systems showing concentration dependent intrinsic diffusivities”. Journal of Molecular Liquids 86 (2000) 69-76
28. D. T. Wadiak, “APPLICATION OF THE FINITE-ELEMENT METHOD TO THE DIFFUSION AND REACTION OF CHEMICAL SPECIES IN MULTILAYERED POLYMERIC BODIES”. Mathematical Modelling, Vol. 7, pp. 385-395, 1986
29. Xiaoyang Liu, et al, “Compressive Properties of Al-Si Alloy Lattice Structures with Three Dierent Unit Cells Fabricated via Laser Powder Bed Fusion” Department of Materials Process Engineering, Graduate School of Engineering, Nagoya

University,Furo-cho, Chikusa-ku, Nagoya 464-8603, Japan

30. J-O Andersson, Thomas Helander,Lars Hdghmd, Pingfang Shi, Bo Sundman, “THERMO-CALC & DICTRA, Computational Tools For Materials Science”. Calphad, Vol. 26, No. 2, pp. 273-312, 2002.
31. Markus J. Buehler, “Predicting mechanical felds near cracks using a progressive transformer difusion model and exploration of generalization capacity” Journal of material research,
32. Yue Wang et al., “Studies of Cu-Sn interdiffusion coefficients in Cu3Sn and Cu6Sn5 based on the growth kinetics”. Scripta Materialia, 10.1016/j.scriptamat.2021.114138.
33. Medvedev, Oleg, “Diffusion Coefficients in Multicomponent Mixtures” technical university of denmark department of chemical engineering,
34. A. Paul, C. Ghogh, W.J. Boettinger, Diffusion parameters and growth mechanism of phase in the Cu-Sn system, Metall. Mater. Trans. A 73 (2011) 92e94.
35. F. Gao, J. Qu, Calculating the diffusivity of Cu and Sn in Cu3Sn intermetallic by molecular dynamics simulations, Mater. Lett. 73 (2012) 92e94.
36. C. Yu, J. Lin, H. Lu, P. Li, J. Chen, First-principles investigation of the structural and electronic properties of Cu6xNixSn5 (x ¼ 0, 1, 2) intermetallic compounds, Intermetallics 15 (2007) 1471e1478.
37. Paul A, Laurila T, Vuorinen V, Divinski SV. Thermodynamics, diffusion and the Kirkendall effect in solids. Springer; 2014.
38. Baird JD. The formation of intermediate alloy layers in the inter-diffusion of metals. J Nucl Energy - Part A React Sci 1960;11(2):81e8.
39. Mirjalili M, Soltanieh M, Matsuura K, Ohno M. TiAl3 formation in the titanium-aluminum diffusion couple, Defect and Diffusion Forum. TransTech Publ; 2012. p. 185e94.
40. A. Paul, C. Ghosh, W.J. Boettinger, Diffusion parameters and growth mechanism of phases in the CueSn system, Metall. Mater. Trans. A 42 (2011)952e963.
41. Laurila, T., Vuorinen, V., & Kivilahti, J.K. (2005). "Interfacial reactions between lead-free solders and common base materials". Materials Science and Engineering: R: Reports, 49(1-2), 1–60.
42. Frear, D.R., Vianco, P.T., & Grivas, D.A. (1994). "Intermetallic formation in the Cu-Sn system". Journal of Electronic Materials, 23(8), 765–771.
43. Hoshino, K., Iijima, Y., & Hirano, K. (1982). Interdiffusion and Kirkendall Effect in Cu–Sn Alloys. Transactions of the Japan Institute of Metals, 21(10), 674–681.
44. Onishi, M., & Fujibuchi, H. (1975). Reaction-Diffusion in the Cu–Sn System. Journal of the Japan Institute of Metals, 39(5), 521–528.
45. Kumar, K. S., et al. (2017). Kinetics of intermetallic phase growth and determination of diffusion coefficients in solid–solid-state reaction between Cu and (Sn+1at.%Ni) pads. Journal of Materials Science, 52(20), 12180–12191.
46. Mei, Z., et al. (2005). Solid state diffusion in Cu–Sn and Ni–Sn diffusion couples with flip-chip scale dimensions. Microelectronics Reliability, 45(3–4), 473–480.
47. Divinski, S., Ribbe, J., Schmitz, G., & Herzig, C. (2007). Grain boundary diffusion and

segregation of Ni in Cu. Acta Materialia, 55(10), 3337–3346.

48. Ph.D. Thesis (2002). Diffusion of nickel through copper twist grain boundaries and influence of diffusion-induced recrystallization on volume diffusion in copper-nickel couples. ADS Abstract
49. IBM Research (1997). Grain boundary diffusion and electromigration in Cu-Sn alloy thin films and their VLSI interconnects. Defect and Diffusion Forum. IBM Research Publication
50. Onishi, M., & Fujibuchi, H. (1975). Reaction-Diffusion in the Cu–Sn System. Journal of the Japan Institute of Metals, 39(5), 521–528.
51. Kumar, K. S., et al. (2017). Kinetics of intermetallic phase growth and determination of diffusion coefficients in solid–solid-state reaction between Cu and (Sn+1at.%Ni) pads. Journal of Materials Science, 52(20), 12180–12191.
52. Larrabee, S. R. (1986). A Study of Diffusion-Induced Grain Boundary Migration (DIGM) in Ni–Sn and Ni–In Alloys. Master's Thesis, Marquette University. Marquette Theses
53. Mei, Z., et al. (2005). Solid state diffusion in Cu–Sn and Ni–Sn diffusion couples with flip-chip scale dimensions. Microelectronics Reliability, 45(3–4), 473–480.